

**AN INVESTIGATION OF ADAPTIVE CONTROL
TECHNIQUES IN OFDM WIRELESS
MODULATION**

By

KRISHNAVENI RAMASAMY

Bachelor of Engineering

Coimbatore Institute Of Technology

India

1999

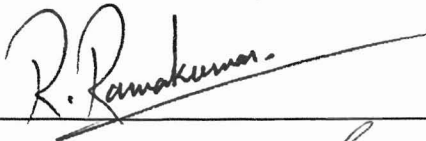
**Submitted to the Faculty of the
Graduate College of the
Oklahoma State University
in partial fulfillment of
the requirements for
the Degree of
MASTER OF SCIENCE
December, 2002**

**AN INVESTIGATION OF ADAPTIVE CONTROL
TECHNIQUES IN OFDM WIRELESS
MODULATION**

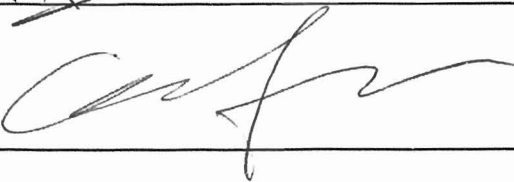
Thesis Approved:



Thesis Advisor



R. Ramakumar



[Signature]



Dean of the Graduate College

ACKNOWLEDGEMENTS

Firstly my sincere thanks are to my advisor Dr. Jong-Moon Chung for his patience, critical suggestions, inspiration, effective guidance, and diligence in helping me through the struggles and without whose help this would have not been possible. I would also like to thank my committee member Dr. Guoliang Fan for the support in the completion of my thesis.

My sincere thanks are also to the Advanced Communication Systems Engineering Laboratory (ACSEL) & Oklahoma Communication Laboratory for Networking and Bioengineering (OCLNB) at the Oklahoma State University for supporting me with the most advanced resources which helped me to achieve my goals efficiently. My gratitude to the OFDM research group for providing vital information in the OFDM area and assisting me with the computer simulations.

My special thanks are to Dr. Ramakumar for serving on my thesis committee and providing much guidance throughout my career at the Oklahoma State University.

Finally, I would like to thank my father, Professor Ramasamy Ellapanaidu, mother, sister, and my brother for their moral support and enthusiasm that I regard most important.

Dedicated to

My dear father,

Prof. Ramasamy Ellapanaidu

“In the time we have it is surely our duty to do all the good we
can to all the people we can in all the ways we can.”

-William Barclay (1907-1978, Scottish Theologian, Religious Writer, Broadcaster)

TABLE OF CONTENTS

Chapter	Page
I. Introduction.....	1
II. Applications of OFDM Systems	
2.1. Wireless Broadband Communications.....	4
2.2. Present and Future Communication Systems.....	5
2.3. MAC Protocols.....	6
III. Technical Review of Single-Carrier & Multi-Carrier Systems	
3.1. Single-carrier, Multicarrier, and OFDM Channel Model.....	8
3.2. OFDM System Representation.....	15
IV. Adaptive Rate, Adaptive Power Modulation Systems	
4.1. Spectral Efficiency of Adaptive M -QAM for continuous rate Adaptation.....	32
4.2. Optimal Power Adaptation.....	37
4.3. Spectral Efficiency of Adaptive M -QAM for discrete rate Adaptation.....	43
4.4. Constant power, Adaptive rate and constant rate, Adaptive power systems.....	45
4.5. BER performance results of the continuous and discrete rate adaptation.....	48
4.6. Observations.....	49
V. Adaptive Modulation for OFDM system and Macroscopic Diversity Techniques	
5.1. Adaptive OFDM	50
5.2. Modulation Parameters in case of Adaptive Modulation of Subcarriers.....	51
5.3. Signaling & Blind Detection.....	54
5.4. Macroscopic diversity.....	56
VI. Conclusions & Future Research.....	66

Appendix-A. Matlab Codes.....	68
References.....	72

CHAPTER 1

INTRODUCTION

Orthogonal Frequency Division Multiplexing (OFDM) is subject to fading and frequency errors, which reduce its usefulness in wireless mobile communication channels. This thesis deals with analyzing the frequency and phase errors and applying adaptive modulation to improve the overall throughput and bit error rate (BER) performance of the OFDM system using adaptive modulation.

Wireless mobile radio channels are subject to both slow and fast fading. Fast fading is caused by the reflected and diffracted signals arriving at the receiver at different times and reducing the signal strength. Goldsmith and Chung [4.1] introduced an adaptive rate and adaptive power modulation control mechanism for capacity improvement at a constant BER performance. Keller and Hanzo [5.3]] introduced an adaptive rate modulation scheme in which OFDM systems are adaptively switched between BPSK¹, QPSK², 16-QAM³ modulations. In this thesis we implement adaptive rate and adaptive power modulation in OFDM systems and apply diversity techniques to further improve the performance. The research also extends the Goldsmith model [4.1] of the adaptive M -QAM approximation technique to reduce the fading and shadowing effects.

¹ BPSK - Binary Phase Shift Keying

² QPSK - Quadrature Phase Shift Keying

³ 16-QAM - 16-Quadrature Amplitude Modulation

The organization of this thesis is as follows. Chapter 2 gives an introduction to the application of OFDM systems. Chapter 3 provides the background information on OFDM and its synchronization technologies. In addition the general definitions of components used in the system model followed by a discussion of channel and effective synchronization procedures are summarized. Adaptive modulation, another key area in improving signal reception of a single carrier system, is discussed in Chapter 4. Additionally, in Chapter 4 the application of variable-rate and variable-power adaptive systems in general and the analysis of their performance when applied to an OFDM systems is investigated in Chapter 5. Following this the shadowed fading channel model is analyzed. To improve the performance due to shadowing effects the macroscopic diversity technique is implemented along with the adaptive system. The results and observations documented in this thesis were generated using Matlab and Mathematica programs by employing Monte Carlo simulations. Chapter 6 summarizes the conclusion of the research and presents areas for future research.

CHAPTER 2

APPLICATIONS OF OFDM SYSTEMS

In this chapter we review the applications and features of practical Orthogonal Frequency Division Multiplexing (OFDM) systems that have been implemented by industry.

OFDM was initially used only in military applications due to its implementation difficulties. Now, it has found new implementations in systems such as IEEE802.11a as well as in the new European satellite-based digital audio/video/terrestrial broadcasting systems [2.1]. In addition, the OFDM-time division multiple access (TDMA) structure has found new applications in wireless Asynchronous Transfer Mode (WATM) providing Broadband Integrated Services Digital Network (B-ISDN) services to mobile users [2.1]. OFDM is considered as one of the cornerstone technologies for next generation wireless systems. New products with higher data rates are now possible through OFDM technology, such as, wireless local area network (WLAN) systems including IEEE 802.11a, European Telecommunications Standards Institute Broadband Radio Access Networks (ETSI BRAN), and new emerging wireless broadband multimedia applications.

2.1. Wireless Broadband Communications

The demand for wireless (mobile) communications as well as Internet/multimedia communications is growing exponentially. While the current systems are primarily designed to provide either voice or multi-media communications, future mobile communication and wireless LAN technology aims at integrating both voice and data services. The next generation Wireless Broadband Multimedia Communications System (WBMCS) aims at a high information rate which requires a careful selection of modulation techniques. One of the emerging wireless broadband networks are the wireless LANs with new systems running in frequency bands above 3GHz.

The frequency bands for wireless broadband communications is as shown in Fig. 2.1. The wireless broadband air access interface channel will demand a relatively large frequency band greater than 2 Mbps, which is easier to accomplish at higher frequencies. Both Europe and the United States have reserved frequency bands for Mobile Broadband Systems (MBSs). Some wireless indoor applications use Orthogonal Frequency Division Multiple Access (OFDMA) in an unlicensed 60 GHz frequency band in support of 155 Mbps data rates. OFDM is used in WATM networks as well with burst transmission. The various projects in the Advanced Communication Technologies and Services (ACTS) program and the parameters used are listed below [2.1]:

Project	WAND	AWACS	SAMBA	MEDIAN
FEC	Complementary coding	Reed-Solomon/BCH	Reed-Solomon	Reed-Solomon (55/71)
Radio access	TDMA/TDD	TDMA/TDD	TDMA/FDD	TDMA/TDD
TDMA slot size	1ATMcell	8ATMc/burst	2ATMc/burst	1ATMc/OFDM
ATM services	CBR, VBR, UBR	CBR, VBR, UBR	CBR, VBR, UBR	CBR, VBR, UBR
Frequency	5 GHz	19 GHz	40 GHz	61.2 GHz
Radio bit rate	20 Mbps	70 Mbps	82 Mbps	155 Mbps
Modulation	OFDM, 16 carriers, 8 PSK	OQPSK/coherent detection	OQPSK	OFDM, 512 carrier, DQPSK
Radio-cell size	20-50 m	50-100 m	1200m, 6000m	10m
Target Environment	Indoor	In/Outdoor	In/Outdoor	Indoor

Table 2.1. Projects in ACTS

The demand for video/voice and data communication over the Internet on mobile phones and Personal Digital Assistant (PDA) are increasing day by day. The application ISM

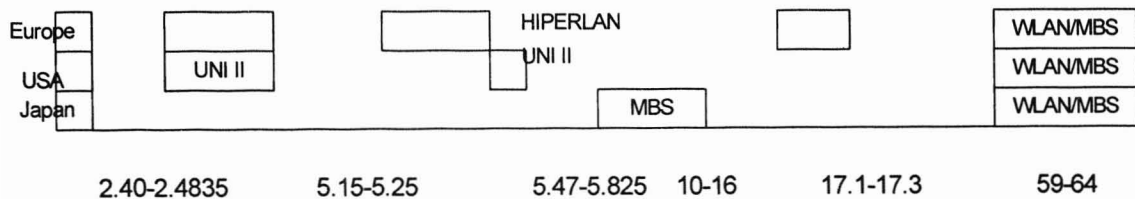


Fig.2.1. Frequency band for wireless broadband communications.

of broadband Internet access on mobile phones is one objective of the research application of this thesis.

2.2. Present and Future Communication System

The third generation (3G) Communication technologies are based on both voice and data communications over mobile telephones at higher data rates at the range of upto 2 Mbps. Wireless Broadband Multimedia Communications Systems (WBMS) technology

is based on integrated services wireless (mobile) communications and Internet/multimedia with an information rate ranging from 2 Mbps to 54 Mbps (IEEE 802.11g/a/b and HIPERLAN systems using frequency bands in the 2 to 60 GHz ranges).

The selection of the modulation and multiplexing technique is critical in determining the performance and efficiency of the system, which led to the research of this thesis on OFDM technology.

2.3. Medium Access Layer Protocols (MAC)

Communications become more difficult when different users share a common transmission medium. Without a protocol to provide coordination and control, all the devices may attempt to transmit simultaneously and the transmission collisions will result in a very low user throughput.

Two possible types of MAC protocols are: 1) Static Allocation Protocols and 2) Dynamic Allocation Protocols.

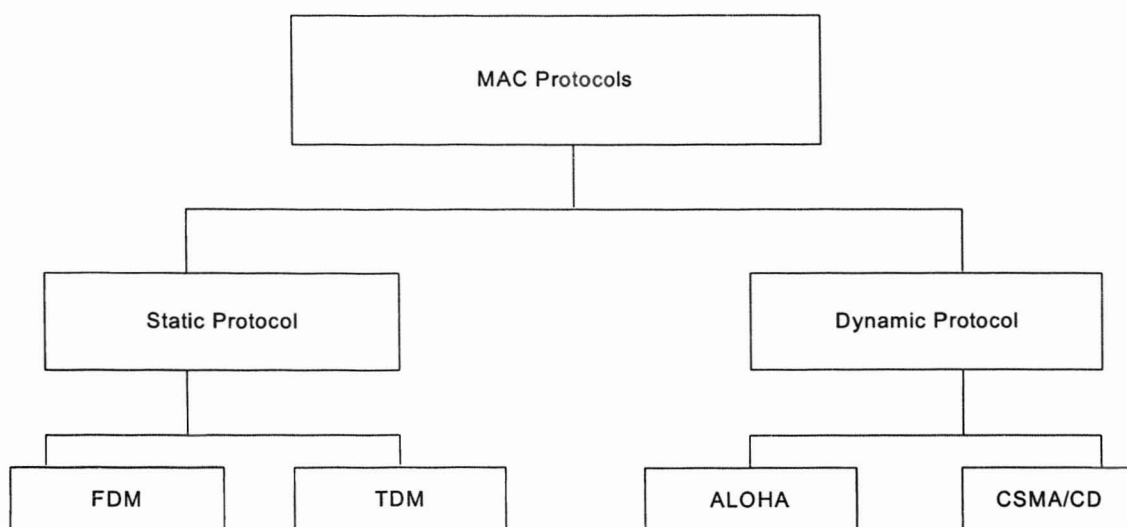


Fig.2.3. Comparing some of the static and dynamic MAC protocols.

Static Allocation protocols include Time Division Multiplexing (TDM) and Frequency Division Multiplexing (FDM) where every user is given a fixed timeslot or frequency band to be used temporarily, and hence the implementation is simpler. Static protocols are most beneficial only when all the users have equal amounts of data to send and are constantly transmitting, thus consuming all of the available bandwidth. Imagine a system with N slices of bandwidth and only M users transmit. In this case, the difference $(N-M)$ slices of bandwidth is not utilized. The situation becomes worse when all the users do not require the same amount of bandwidth. The Dynamic Allocation Protocol assigns bandwidth on an as-needed basis, which is a better topology in the case of the non-uniform transmission data rate and user characteristics. Random access protocols, which are a part of the dynamic allocation protocols, include ALOHA, Slotted ALOHA and Carrier Sense Multiple Access with Collision Detection (CSMA/CD) MAC techniques. The Slotted ALOHA Protocol gives an efficient means of access for OFDM techniques.

CHAPTER 3

TECHNICAL REVIEW OF SINGLE-CARRIER AND MULTI-CARRIER SYSTEMS

In this chapter the mathematical structure of OFDM systems and channel performance characteristics are presented.

This chapter is divided into the following sections. In the first section, a comparison of single-carrier and multicarrier systems in terms of BER performance and channel characteristics are studied. Further, we analyze the performance of these systems in a Gaussian and non-Gaussian environment. The basic OFDM system is modeled in this chapter. Four main criteria are used to assess the performance of the OFDM system; they are: tolerance to multipath delay spread, peak power clipping, channel noise, and time synchronization errors. Further, the OFDM mathematical representation model with the fading characteristics is also studied. The probability of failure of frequency synchronization, which is a main criterion in determining the orthogonality of the system, is also calculated.

3.1. Single-Carrier, Multi-Carrier and OFDM Channel Model

Selection of the modulation technique employed in wireless systems plays an important role in determining system cost and efficiency. Some of the recent equipment manufacturers are using OFDM in place of Single-Carrier systems (SC) due to the reason that OFDM has a higher efficiency than SC systems. The use of OFDM is advantageous

because it removes the intersymbol interference (ISI) if the delay spread is less than the guard band. IEEE802.11a WLANs OFDM is used with an 800 ns of cyclic prefix to eliminate the multipath delay spread. Although research is going on in this field, most of the papers in the literature do not give analytical comparisons of different systems. In this section, SC to multicarrier modulation and OFDM modulation techniques in Gaussian and Rayleigh channels are analyzed.

1) Statistical Models for Multipath Fading channels

The communication environment under study is a multipath fading channel. The transmitted signal, when transmitted, depending on the propagation area and multipath profile, will arrive at the receiver at different times. These signals sometimes may add up or sometimes become nullified. When the signal is nullified it is said that fading has occurred.

2) Single carrier systems

In a single carrier system with the carrier frequency represented by f_c , the transmitted signal $s(t)$ can be represented as [3.1]

$$s(t) = \text{Re} \left[s_I(t) e^{j2\pi f_c t} \right] \quad (3.1)$$

Here, $s_I(t)$ represents the complex form of the transmitted signal. The received signal with the attenuation factor and the phase shift due to fading is given by,

$$r(t) = \text{Re} \left\{ \left[\sum_n \alpha_n(t) e^{-j2\pi f_c \tau_n(t)} s_I(t) \right] e^{j2\pi f_c t} \right\}$$

$$= \sum_n \alpha_n(t) e^{-j2\pi f_c r_n(t)} s_l(t) \cos 2\pi f_c t$$

The equivalent lowpass channel is represented as

$$\begin{aligned} h(t) &= \sum_n \alpha_n(t) e^{-j2\pi f_c t_n(t)} \delta(t) \\ &= \sum_n \alpha_n(t) e^{-j2\pi f_c t_n(t)} \\ &= \sum_n \alpha_n(t) \cos 2\pi f_c t_n(t) - j \sum_n \alpha_n(t) \sin 2\pi f_c t_n(t) \\ &= X_1(t) + X_2(t), \end{aligned}$$

where $X_1(t)$ and $X_2(t)$ are two zero-mean Gaussian random variables. The amplitude and phase of the received signal are given by, $Ra(t) = \sqrt{X_1(t)^2 + X_2(t)^2}$ and $\theta(t) = \tan^{-1}(X_2(t)/X_1(t))$, respectively [3.4].

The Rayleigh distribution is mostly used as a channel distribution model for multipath fading in mobile channels. The power distribution is closely related to a chi-square distribution given by $Ra = X_1^2 + X_2^2$ where X_1 and X_2 are two zero-mean Gaussian random variables with variance σ^2 . Since the result is a chi-square distribution with two degrees of freedom, the general probability density function can be represented as [3.4]

$$f_R(r) = \frac{2r^{n-1}}{2^{n/2} \sigma^n \Gamma(n/2)} e^{-\frac{r^2}{2\sigma^2}} U(r) \quad (3.2)$$

The probability density function for the same are given by

$$f_R(r) = \frac{r}{\sigma^2} e^{-\frac{r^2}{2\sigma^2}}, \quad r > 0 \quad (n = 2, \Gamma(n-2) = (n-2)! = 1, \text{ for } n > 0)$$

$$f_{\theta}(\theta) = \frac{1}{2\pi}, \quad -\pi \leq \theta \leq \pi \quad (3.3)$$

The graph below shows the probability density function of the Gaussian and Rayleigh density of a single carrier system.

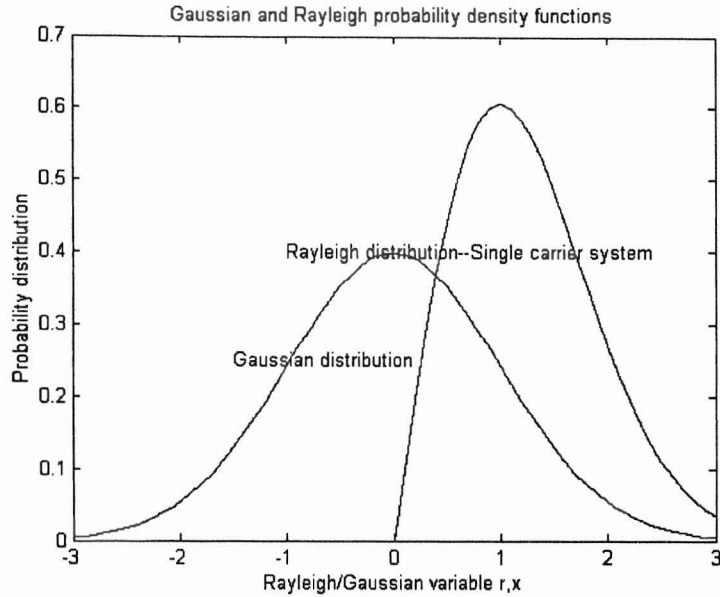


Fig.3.1. Probability Distribution Function of a SC system.

Probability of error: The probability of bit error for a BPSK system in an AWGN channel is given by the equation (3.4), (based on a signal-to-noise ratio represented by $\frac{E_b}{N_o}$). The noise is assumed to follow the Gaussian distribution function with variance a of $N_o / 2$.

$$P_b = \text{erfc}\left(\sqrt{\frac{2E_b}{N_o}}\right) = \text{erfc}(\sqrt{\gamma_b}) \quad (3.4)$$

To find the communication system probability of bit error in a Rayleigh fading channel [3.1], the probability of error is integrated over the Rayleigh distribution function as shown below:

$$\begin{aligned}
 P_{br} &= \int_0^{\infty} P_b(\gamma_b) f_{\gamma_b}(\gamma_b) d\gamma_b \\
 P_{br} &= \int_0^{\infty} \text{erfc} \sqrt{\gamma_b} \left(\frac{1}{\gamma_b} e^{-\frac{\gamma_b}{\gamma_b}} \right) d\gamma_b \\
 &= \frac{1}{2} \left(1 - \sqrt{\frac{\gamma_b}{1 + \gamma_b}} \right)
 \end{aligned} \tag{3.5}$$

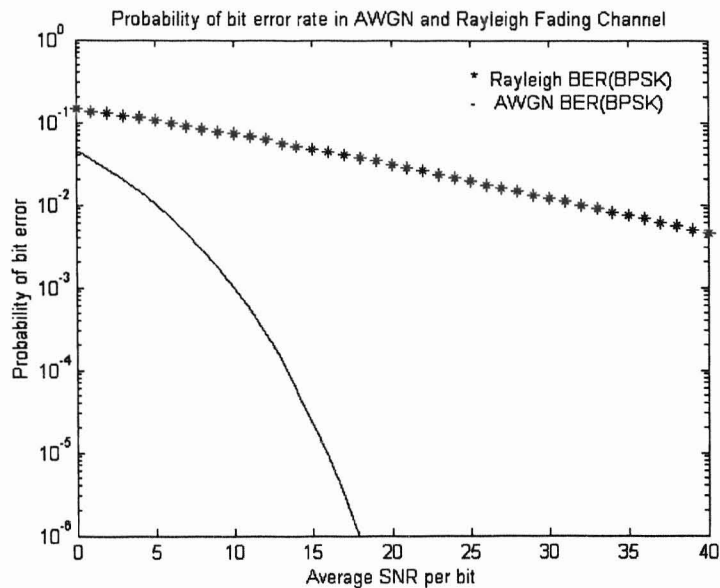


Fig.3.2. Performance of BER on a single-carrier Rayleigh fading channel.

where $f_{\gamma_b}(\gamma_b)$ is the probability function of the SNR, which is $\left(\frac{1}{\bar{\gamma}_b}\right)e^{-\frac{\gamma_b}{\bar{\gamma}_b}}$ where

$\bar{\gamma}_b$ denotes the average SNR.

The performance graph of the single carrier BPSK signal in a fading channel (Fig.3.2) shows that fading introduces a significantly higher BER compared to AWGN channels. From Fig.3.2, we observe that for a bit error rate of 0.01 approximately a 25dB gain in the signal to noise ratio is required for the system to perform equivalently in Rayleigh fading channels.

3) Single-Carrier and Multicarrier M -QAM systems

Performance of M -QAM in a non-Gaussian environment: The performance of most of the M -QAM digital communication systems is based on a Gaussian environment. But, in actual situations, the noise model must also include various man-made interference factors, as well as shadowing and multipath fading effects. Non-Gaussian noise can be characterized as large impulses occurring at the detection interval.

The transmitted signal is given by:

$$s(t) = \text{Re}\left[s_l(t)e^{jw_c t}\right]$$

$$s_l(t) = \sum_{k=-\infty}^{\infty} (A_k + jB_k)a(t - kT),$$

where $a(t)$ is the low-pass shaping pulse and T is the symbol duration. $(A_k + jB_k)$ corresponds to the complex symbol transmitted during the k^{th} symbol interval.

Noise model: The noise model is represented by two factors: the AWGN noise $n_0(t)$ and the impulse noise $n_\beta(t)$. Combining the two factors together we obtain

$$n(t) = n_0(t) + n_\beta(t) = \text{Re}\{[n_{0l}(t) + n_{\beta l}(t)]e^{j\omega_c t}\}, \quad (3.6)$$

where $n_{0l}(t)$ is the complex envelope of $n_0(t)$ and $n_{\beta l}(t)$ is the complex envelope of $n_\beta(t)$. At the receiver, the noise vector n is defined by two complex random variables as shown in (3.7).

In our model, we take the analysis with these impulse noise terms following a Rayleigh distribution in the fading environment.

The probability distribution function and hence the probability of BER is given by [3.1],

$$f_R(r) = e^{-\gamma} \sum_{k=0}^{\infty} \frac{\gamma^k}{k!} \frac{r}{\sigma_n^2} e^{\frac{-r^2}{2\sigma_n^2}} u(r)$$

$$\sigma_n^2 = \sigma_{n_0}^2 + \frac{k}{\gamma} \sigma_{n_\beta}^2$$

$$P_e = 4e^{-\gamma} \sum_{k=0}^{\infty} \frac{\gamma^k}{k!} \left(1 - \frac{1}{K}\right) P_n \left[\left(1 - \frac{1}{K}\right) P_n \right]$$

$$P_n = \frac{1}{2} \text{erfc} \left(\sqrt{\frac{3}{2(M-1)} \frac{E_a}{\sigma_n^2}} \right) \quad (3.7)$$

$$\beta = \frac{\sigma_{n_0}^2}{\sigma_{n_\beta}^2}.$$

Let $\sigma_{n_\beta}^2$ represent the impulsive noise variance and let $\sigma_{n_0}^2 = (N_0/2)$ represent the two-sided Gaussian noise variance. The modulus of the real and imaginary components of the

non-Gaussian random variable is represented as $r = \sqrt{X^2 + Y^2}$, and γ is the distribution parameter.

The term $\beta = \frac{\sigma_{n_0}^2}{\sigma_{n_\beta}^2}$ is the factor that determines the ratio of the impulsive noise power

and Gaussian power, which plays an important role in the performance analysis of single-carrier M -QAM systems. The first-order approximations and the quasi-Gaussian approximations of the AWGN channel are compared with the results from the Rayleigh distribution in Fig.3.3.

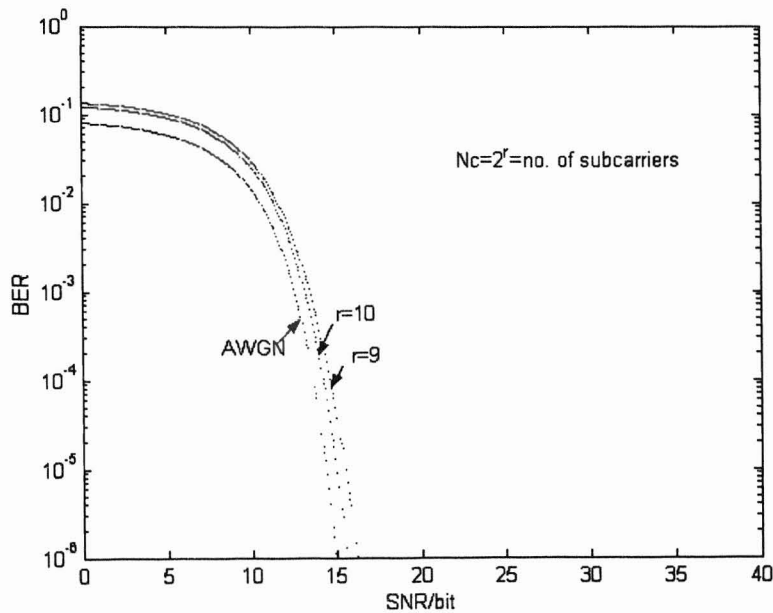


Fig.3.3. Performance of Rayleigh fading system.

3.2. OFDM System Representation

1) Mathematical Representation of OFDM Systems

In case of multipath signal propagation, different signals arrive at different times. This leads to a delay spread of the channel, which causes intersymbol interference (ISI).

OFDM is an orthogonal multiplexing technique used to eliminate ISI by using guard bands. This section gives an introduction to the multicarrier modulation implemented in the OFDM system using Fast Fourier Transform (FFT) and Inverse Fast Fourier Transform (IFFT).

Multicarrier modulation (MCM) reduces the interference effects induced on single-carrier systems. The analysis is the same as the previous section with the white noise characterized by the Gaussian distribution and the impulsive noise characterized by Rayleigh distribution. All the sub-carriers exhibit the same modulation level M .

MCM is a parallel transmission technique where the bit stream to be transmitted is divided into equal length symbols applying N_c number of carriers. Using the IFFT modulator, the received sample r_k , in terms of transmitted sample and noise factor n_k , is given by

$$r_k = \frac{1}{\sqrt{N_c}} \sum_{n=0}^{N_c-1} s_n e^{\frac{-j2\pi nk}{N_c}} + n_k \quad \text{for } k = 0, \dots, N_c - 1.$$

The received sample after FFT is given by $\frac{1}{\sqrt{N_c}} \sum_{n=0}^{N_c-1} r_k e^{\frac{-j2\pi nk}{N_c}}$.

The probability distribution function of the noise random variable is given by,

$$f_R(r) = \frac{e^{-\gamma N_c}}{2\pi} \sum_{k=0}^{\infty} \frac{(\gamma N_c)^k}{\left(\sigma_{n_0}^2 + \frac{k}{\gamma N_c} \sigma_{n_\beta}^2\right)} e^{-\frac{r^2}{2\left(\sigma_{n_0}^2 + \frac{k}{\gamma N_c} \sigma_{n_\beta}^2\right)}}.$$

The M -QAM/MCM technique has a similar effect to the SC-QAM except that the distribution parameter γ is replaced by the multiplicative term of the number of

subcarriers N_c . The equation below represents the probability of error for a multicarrier system.

$$P_e = 4e^{-\gamma N_c} \sum_{k=0}^{\infty} \frac{(\gamma N_c)^k}{k!} \left(1 - \frac{1}{\sqrt{M}}\right) P_k \left[\left(1 - \frac{1}{\sqrt{M}}\right) P_k \right]$$

where the term P_k is given by

$$P_k = \frac{1}{2} \operatorname{erfc} \left(\sqrt{\frac{3}{2(M-1)} \frac{E_a}{\sigma_k^2}} \right),$$

$$\sigma_k^2 = \sigma_G^2 + \frac{k}{\gamma N_c} \sigma_I^2.$$

The term σ_k^2 is based on two noise variance factors, $\sigma_G^2 = \sigma_{n_0}^2$ and $\sigma_I^2 = \sigma_{n_\beta}^2$.

In case of a multicarrier system, increasing the number of carriers decreases the impulsive component $\beta = \frac{\sigma_{n_0}^2}{\sigma_{n_\beta}^2}$. In case of low β , the performance reaches AWGN as the number of carriers increase. When $\beta \gg \gamma N_c$, the noise is highly impulsive. This shows that with an increase in number of carriers, the Gaussian BER performance can be closely approached by the multicarrier system. The structure of an OFDM system is provided in Fig.3.4.

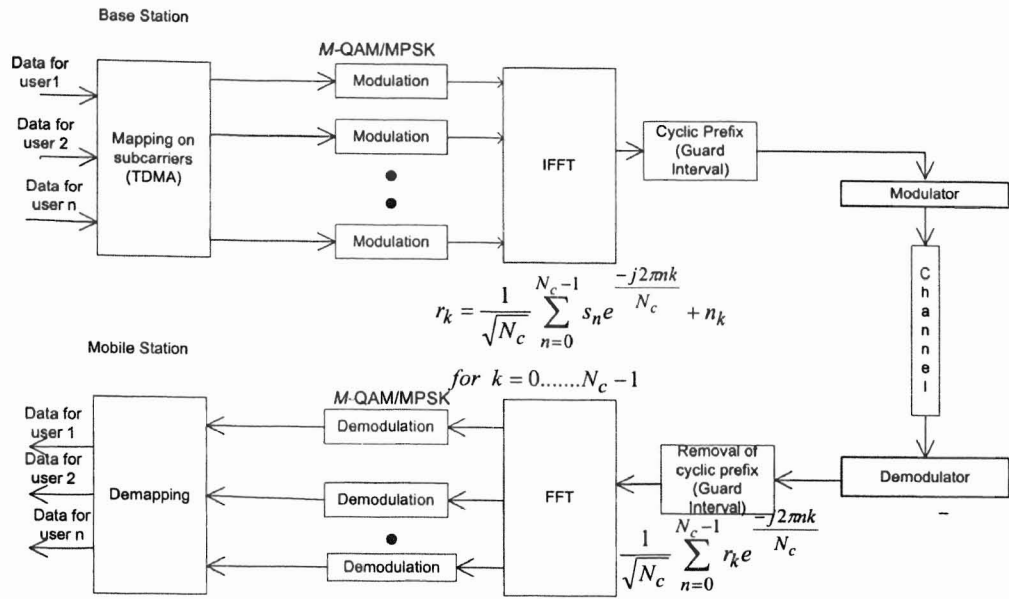


Fig.3.4. OFDM System Model

a) Serial to Parallel Conversion: In the system shown in Fig.3.4, the input serial data stream is formatted into the word size required for transmission, e.g., 2bit/word for QPSK, 1bit/word for BPSK and shifted into a parallel format. The data are then transmitted in parallel by assigning each data word to one carrier in the transmission.

b) Modulation of Data: The modulation techniques commonly used in OFDM are either M -QAM (Quadrature Amplitude Modulation with M number of constellations) or M -PSK (Phase Shift Keying) systems. The data to be transmitted on each carrier are differentially encoded with previous symbols then mapped into a PSK or QAM format. Since differential encoding requires an initial phase reference an extra symbol is added at the start for this purpose. The data on each symbol are then mapped to a phase angle based on the modulation method. For example, in QPSK the phase angles used are 45° , 135° , 225° , and 315° .

c) Inverse Fast Fourier Transform: After the required spectrum is worked out, an inverse fast Fourier transform (IFFT) is used to find the corresponding time waveform. The guard period is then added to the start of each symbol.

d) Guard Period: The guard period is a cyclic extension of the symbol to be transmitted. This is to allow for symbol timing to be easily recovered by envelope detection and helps avoid interchannel interference (ICI). After the guard period has been added, the symbols are then converted back to a serial time waveform. This becomes the baseband signal for the OFDM transmission system.

e) Channel: The transmitted signal then passes through the radio channel. This radio channel is modeled as a scatter communication channel. The receiver is designed with the multitude of reflected and delayed signal components. These signals tend to reinforce or cancel each other. This results in fading. This channel model is characterized by a lognormally shadowed Rayleigh fading model (described later in this chapter) undergoing multipath delay spread shadowing. A feedback link is also available which informs the receiver about the channel conditions and hence make some changes in the transmission parameters of the signal.

f) Receiver: The receiver basically does the reverse operation of the transmitter. After demodulating the signal from the transmission band, the guard period is removed from the data/voice symbol. The FFT of each symbol is then taken to find the original transmitted signal. The phase angle of each transmission carrier is then evaluated and

converted back to the data word by demodulating the received phase. The data words are then combined back to the same word size as the original data.

2) Application of Rayleigh fading characteristics on an OFDM system

Orthogonal frequency division multiplexing uses guard intervals to eliminate the intersymbol interference between data blocks. But, since the channel undergoes time variations, there is a loss of subchannel orthogonality. If the bandwidth of the channel is larger than the coherence bandwidth, then the channel is a non-frequency selective fading channel. If T_m is the delay spread of the channel, then the coherence bandwidth for the channel is termed as $1/T_m = B_d$. In case of frequency selective channel, the effective bandwidth of the channel is less than the coherence bandwidth.

The same procedure applied to calculate the destruction introduced due to a single carrier system is also employed in multicarrier OFDM systems which can be denoted as follows:

Let the received signal be given as

$$\begin{aligned}
 R_k &= \alpha S_k + \beta_k + N_k \\
 \alpha &= \frac{1}{N} \sum_{i=0}^{N-1} |h_i| = \frac{1}{N} \left(\frac{N}{2} (|h_0| + |h_{N-1}|) \right) \\
 &= \frac{1}{2} (r_0 + r_{N-1}).
 \end{aligned} \tag{3.8}$$

The Rayleigh fading envelope of r_0 is given by,

$$f_R(r_0) = \frac{r_0}{\sigma^2} e^{-\frac{r_0^2}{2\sigma^2}}, r_0 > 0$$

Similarly, the Rayleigh faded envelope for sample r_{N-1} can be written as,

$$f_R(r_{N-1}) = \frac{r_{N-1}}{\sigma^2} e^{-\frac{r_{N-1}^2}{2\sigma^2}}, \quad r_{N-1} > 0.$$

The joint probability function of the two sample points can be represented by the density equation,

$$f_R(r_0, r_{N-1}) = \frac{r_0 r_{N-1}}{\sigma^4 (1-\lambda^2)} e^{-\frac{r_0^2 + r_{N-1}^2}{2\sigma^2 (1-\lambda^2)}} I_0\left(\frac{\lambda r_0 r_{N-1}}{\sigma^2 (1-\lambda^2)}\right), \quad r_0, r_{N-1} > 0.$$

Substituting from (1), the probability density function (PDF) of α becomes,

$$f_\alpha(\alpha) = 2 \int_0^{2\alpha} \frac{(2\alpha - r_{N-1}) r_{N-1}}{\sigma^4 (1-\lambda^2)} e^{-\frac{(2\alpha - r_{N-1})^2 + r_{N-1}^2}{2\sigma^2 (1-\lambda^2)}} I_0\left(\frac{\lambda(2\alpha - r_{N-1}) r_{N-1}}{\sigma^2 (1-\lambda^2)}\right) dr_{N-1}, \quad r_{N-1} \geq 0.$$

The overall bit error rate for the BPSK modulated OFDM signal is given by,

$$\begin{aligned} P_{br} &= \int_0^\infty \operatorname{erfc}\left(\sqrt{\frac{\alpha^2 E_s}{\sigma_\beta^2 + N_o/2}}\right) f_\alpha(\alpha) d\alpha \quad (3.9) \\ &= 2 \int_0^\infty \int_0^{2\alpha} \frac{(2\alpha - r_{N-1}) r_{N-1}}{\sigma^4 (1-\lambda^2)} e^{-\frac{(2\alpha - r_{N-1})^2 + r_{N-1}^2}{2\sigma^2 (1-\lambda^2)}} I_0\left(\frac{\lambda(2\alpha - r_{N-1}) r_{N-1}}{\sigma^2 (1-\lambda^2)}\right) \operatorname{erfc}\left(\sqrt{\frac{\alpha^2 E_s}{\sigma_\beta^2 + N_o/2}}\right) dr_{N-1} d\alpha \end{aligned}$$

where $N_o/2$ represents the Gaussian noise density, σ_β^2 gives the ICI noise power, and $\alpha^2 E_s$ is the effective signal strength after fading.

3) OFDM Frame Synchronization

Synchronization is an important factor of OFDM modulation. Since the OFDM system performance is highly dependent on maintaining the orthogonality of the carriers, avoiding intercarrier interference (ICI) and intersymbol interference (ISI) becomes an important factor. The receiver needs to know the exact position of the subcarriers in order for the system to be in synchronization with the transmitter. The synchronization error as a result may lead to two types of effects: frequency offset or phase error. The frequency and phase jitter introduced in the system leads to the displacement of the subcarriers being separated by exact intervals thus causing ICI and ISI.

Comparison of single-carrier Systems and multicarrier Systems in terms of interference: For single carrier systems, phase noise and frequency offsets introduce degradation to the performance. The sensitivity of phase noise and frequency offset has a greater effect on multicarrier systems than single-carrier systems, which is one of the disadvantages of OFDM relative to single-carrier systems.

Degradation in multicarrier systems (OFDM): This section discusses the degradation introduced due to phase noise and frequency offset.

An OFDM signal consists of N sinusoids (bins), which are orthogonal and are spaced T seconds apart. The effect of frequency offset and phase error in terms of the variance of the noise terms is calculated as [3.2]

$$\sigma_v^2 = E\left[|\delta|^2\right] + \sum_{\substack{m=0 \\ m \neq k}}^{N-1} E\left[|I_{k-m}|^2\right] \quad (3.10)$$

In (3.10), the term $E\left[|\delta|^2\right]$ results from the additional noise component, whereas

$\sum_{\substack{m=0 \\ m \neq k}}^{N-1} E\left[|I_{k-m}|^2\right]$ represents the interbin interference noise variance caused due to other

bins interfering with the k^{th} bin.

As $E\left[|I_m|^2\right]$ decreases with increasing m , we can approximate σ_v^2 as

$$\sigma_v^2 \approx E\left[|\delta|^2\right] + \sum_{\substack{m=0 \\ m \neq k}}^{N-1} E\left[|I_{k-m}|^2\right] \approx \sum_{m=-\infty}^{+\infty} E\left[|I_m|^2\right] - E_1,$$

where $E_1 = E\left[|I_0|^2\right]$. Let T represent the symbol duration. When there exists a

frequency offset given by Δf , then $|I_0| = \frac{\sin(\pi\Delta f T)}{\pi\Delta f T}$.

$$\sum_{m=-\infty}^{+\infty} E\left[|I_m|^2\right] - E_1 = 1 - E_1$$

$$= 1 - E_1$$

$$E\left[|\delta|^2\right] = E_1 - E_0^2$$

where E_0^2 is the power of the useful component. Therefore, the variance of other noise

terms is given by

$$\sigma_v^2 = E_1 - E_0^2 + 1 - E_1 = 1 - E_0^2. \quad (3.11)$$

Sensitivity of Signal to Noise Ratio due to Frequency offset: The OFDM symbols use FFT technique for frequency modulation techniques. The frequency carriers of this OFDM symbol should be an integer number of cycles in the FFT interval. The effect of frequency offset introduces the carriers to be no longer an integer multiple of FFT interval. Hence, ICI is introduced into the system thus reducing the SNR.

The detailed calculation are discussed below. The following BER sensitivity of OFDM systems to Carrier Frequency Offset and Weiner Phase Noise leads to finding the probability of failure of synchronization. Let l be the number of the OFDM symbol with k number of subcarriers. The resulting OFDM signal can be written as (without noise and static frequency offset),

$$r_{l,k} = a_{l,k} \text{sinc}(\pi \Delta f T_u) H_{l,k},$$

where T_u is the OFDM symbol period, $H_{l,k}$ is the transfer function for the Rayleigh frequency selective fading channel with a maximum dispersion of $\tau_{\max} \leq \Delta$ represented by the equation,

$$H_{l,k} = \sum_i h_i(t) e^{2\pi i \frac{k}{T_u}}$$

The FFT signal output for the symbol can be written as,

$$r_{l,k} = a_{l,k} I_0 + \sum_{\substack{n=0 \\ n \neq k}}^{N-1} a_{l,n} I_{k-n} + n_{l,k}$$

$$I_0 = E_0 + \delta$$

where $E_0 = E[|I_0|]$ contributes for the useful component of the signal and δ is the noise component. The degradation can be defined as the SNR without phase error and frequency offset to the SNR with the influence of error.

$$SNR_{\text{without-frequency-offset}} = \frac{E_s}{N_0}$$

$$SNR_{\text{with-frequency-offset}} = \frac{E_0^2}{\frac{N_0}{E_s} + \sigma_v^2}$$

$$\text{Degradation} = \frac{SNR_{\text{without-frequency-offset}}}{SNR_{\text{with-frequency-offset}}} = \frac{\frac{E_s}{N_0}}{\frac{E_0^2}{\frac{N_0}{E_s} + \sigma_v^2}} = \frac{1}{\frac{E_0^2}{E_s} + \sigma_v^2 \left(\frac{E_s}{N_0}\right)}$$

Taking the logarithm on both sides we get,

$$D(\text{db}) \approx \frac{10}{\ln 10} \left((1 - E_0^2) + \sigma_v^2 \left(\frac{E_s}{N_0}\right) \right),$$

which corresponds to the degradation caused due to frequency offset.

Noise power due to static frequency errors σ_v^2 is derived from equation (3.11) as

$$\sigma_{\Delta f}^2(l, k) = 1 - E_1 = 1 - E_0^2 = 1 - |I|^2 \approx 1 - \left(1 - \frac{(\pi \Delta f T_u)^2}{3}\right) = \frac{(\pi \Delta f T_u)^2}{3} \quad (3.13)$$

With the static frequency, the receiver is phase rotated which in turn leads to ICI.

$$D_{\text{freq}} \cong \frac{10}{3 \ln 10} (N \pi \Delta f T)^2 \frac{E_s}{N_o} \quad (3.14a)$$

$$D_{\text{freq}}^{MC} \cong \frac{10}{3 \ln 10} (N \pi \Delta f T)^2 \frac{E_s}{N_o} \quad (3.14b)$$

The equation (3.14a) represents the degradation introduced in case of single-carrier systems and the equation (3.14b) gives the degradation of a multicarrier system where N represents the number of subcarriers in the system.

The graph below shows the degradation introduced due to frequency offset based on the equation (3.14a).

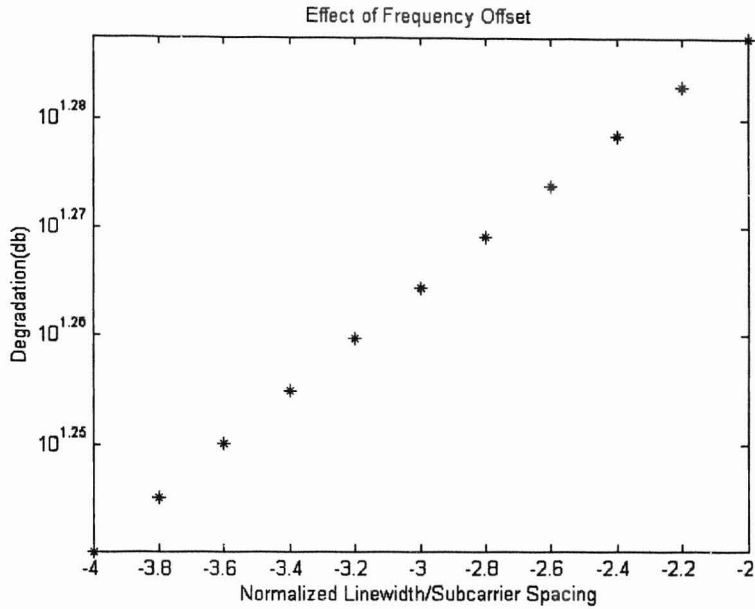


Fig.3.5. Effect of Degradation due to Frequency Offset

Sensitivity to Phase Error: Phase Offset in an OFDM system leads to two effects. The first effect is that a phase offset leads to a random phase error and in such cases the oscillator linewidth is much smaller than the OFDM symbol rate leading to correlation from symbol to symbol. The amount of degradation compared to the original signal strength is calculated as follows. Sensitivity to phase noise is given by [3.2]

$$D_{phase} \cong \frac{11}{6 \ln 10} 4\pi\beta T \frac{E_s}{N_o} \quad (3.14)$$

This is derived from [3.2] as indicated below:

From equation (3.11) and according to experimental results it is proved that the variance

$\sigma_{\text{phase-noise}}^2$ in case of phase noise is given by,

$$E_1 = 1 - \frac{1}{6}(4\pi\beta T) = E_0^2$$

$$\sigma_{\text{phase-noise}}^2 = \frac{1}{6}(4\pi\beta T).$$

We obtain the degradation due to phase noise as,

$$D_{\text{freq}} \cong \frac{10}{6 \ln 10} (4\pi\beta T)^2 \frac{E_s}{N_o} \quad (3.16)$$

Impact of Symbol Timing Error: At the receiver, the guard interval is removed and then Fast Fourier Transform is processed to the OFDM symbol. In order to identify the exact occurrence of the OFDM symbol, there should not be any timing offset. The introduction of timing offset in an OFDM signal leads to the disturbance of the subcarrier symbol defined by

$$r_{l,k} = e^{j2\pi \frac{n_\epsilon}{N}} \frac{N - n_\epsilon}{N} a_{l,k} H_{l,k} + n_{n_\epsilon}(l, k). \quad (3.17)$$

The noise power due to the timing offset can be calculated by the autocorrelation of the symbols given by,

$$\begin{aligned}
\sigma_{n_\varepsilon}^2 &= \left(\frac{n_\varepsilon - \frac{\tau_i}{T}}{N} \right) \left(\frac{N - \left(n_\varepsilon - \frac{\tau_i}{T} \right)}{N} \right) \\
&= \frac{1}{N} \left(n_\varepsilon - \frac{\tau_i}{T} \right) - \frac{1}{N^2} \left(n_\varepsilon^2 - 2 \frac{n_\varepsilon \tau_i}{T} + \frac{\tau_i^2}{T} \right) \\
&= \frac{1}{N} \Delta \varepsilon_i - \frac{1}{N^2} \Delta \varepsilon_i^2,
\end{aligned}$$

where $\Delta \varepsilon_i = n_\varepsilon - \frac{\tau_i}{T}$.

4) Probability of failure of frequency synchronization

The noise terms (thermal noise distribution σ_N^2 along with other noise terms $\sigma_{error(l,k)}^2$) of the signal can be represented as $\sigma_N^2 + \sigma_{error(l,k)}^2$. Hence, the signal-to-noise ratio can be given by

$$\text{SNR} = \frac{E_0^2}{\sigma_N^2 + \sigma_{error(l,k)}^2}.$$

where l is the number of the OFDM symbol and k is number of subcarriers.

The resulting OFDM received signal can be written as (with noise due to frequency offset and phase error) can be given by $z_{l,k}$ [3.3]

$$z_{l,k} = e^{j2\pi\Delta f l(T_s)} a_{l,k} \text{sinc}(\pi\Delta f T_u) H_{l,k} + N_{l,k} + n_{\Delta f}(l,k) + n_{\text{phaseoffset}}(l,k).$$

The average power of the channel noise is given by the factor $N_{l,k}$, whereas $n_{\Delta f}(l,k), n_{\text{phaseoffset}}(l,k)$ constitute the noise variance due to frequency and phase offset error and its sum is given $\sigma_{\text{error}(l,k)}^2$.

The Probability of failure of symbol synchronization is determined by the condition,

$$\sigma_{\text{error}(l,k)}^2 < \frac{1}{K} \sigma_N^2 \text{ where } K \text{ is a constant depending on channel conditions.}$$

Time and frequency synchronization is a critical performance measure of OFDM systems. Various synchronization procedures are followed to reduce the above synchronization error. In this thesis, we assume that we have perfect synchronization between the transmitter and receiver.

In order to improve the overall performance of the OFDM system, OFDM Adaptive modulation is employed to improve the optimization of the power transmission and effective modulation techniques (which is discussed in the coming chapters).

CHAPTER 4

ADAPTIVE RATE, ADAPTIVE POWER MODULATION SYSTEM

In this chapter, we discuss the bit error rate performance and spectral efficiency of an adaptive rate and adaptive power system which was presented in Goldsmith and Chung [4.1].

Adaptive modulation is one of the key areas of research currently under investigation to maximize the capacity and performance of wireless systems. The mobile channels under investigation suffer from deep fades due to multipath signals arriving at the receiver. Choosing the highest modulation scheme that will give the best BER could maximize the spectral efficiency of these communication channels. Using adaptive modulation, the carrier modulation is matched to SNR, maximizing the overall spectral efficiency (in bps/Hz) of the channel. A Time Division Duplex Channel (TDD) (feedback channel) is used in order to appropriately determine channel conditions during the next time slot for the transmitter to select the required modulation levels for its subcarriers.

High-speed wireless communication applications require a system with high spectral efficiency. In a non-adaptive system, it is required that the system be designed for worst or average channel conditions. Since the wireless channel characteristics are dynamic, in case the channel quality gets worse, the channel capacity will not be utilized effectively. When the channel is estimated and the information is transmitted back to the transmitter, the power and transmission rate can be adapted to make best use of the

channel conditions and hence produce a better system performance compared to fixed wireless systems. In [4.1], the spectral efficiency of variable-rate and variable power adaptive systems applying M -QAM is studied showing that the adaptive system results in an improved performance.

The analysis is carried out for two types of systems – continuous and discrete. An ideal adaptation system is the continuous rate adaptation using infinite modulation levels. The discrete rate adaptation is the one that can be implemented in a practical system. It takes finite levels of modulation index changes. The following sections describe these two types of adaptations and their spectral efficiency in an M -QAM system.

4.1. Spectral Efficiency of Adaptive MQAM for continuous rate adaptation

In order to analyze adaptive modulation techniques using optimal power and rate adaptation, the BER equation for M -QAM in [4.1] has to be approximated to a more differentiable form as given below in this section.

The following adaptation analysis is done for single-carrier modulation. Let M represent the number of constellation levels with $M = 2^k$, where k gives the number of bits/symbol used in the modulation.

With Gaussian noise of N_0 , let $\frac{E_{av}}{N_0}$ represents the average signal to noise ratio.

From Proakis [2.1], the probability of BER can be calculated as follows,

$$P_{\sqrt{M}} = 2 \left(1 - \frac{1}{\sqrt{M}} \right) \operatorname{erfc} \left(\sqrt{\frac{3}{M-1} \frac{E_{av}}{N_0}} \right). \quad (4.1)$$

Assuming Gray-bit mapping, Substituting $M = 2^k$ in (4.1), the probability of bit-error rate can be obtained by the equation, $P_b = \frac{1}{k} P_M$, resulting in

$$\begin{aligned}
 BER_{M - \text{QAM}} &\approx \frac{1}{k} P_M \\
 &\approx \frac{1}{k} \left[1 - \left(1 - \left(2 \left(1 - \frac{1}{\sqrt{2^k}} \right) \text{erfc} \left(\sqrt{\frac{3}{2^k - 1} \frac{E_{av}}{N_0}} \right) \right)^2 \right) \right] \\
 &\approx \frac{2}{k} \left(\left(1 - \frac{1}{\sqrt{2^k}} \right) \text{erfc} \left(\sqrt{\frac{1.5}{2^k - 1} \frac{E_{av}}{N_0}} \right) \right).
 \end{aligned}$$

Since this function cannot be easily differentiated, the above BER equation is converted to a more easily differentiable form based on [4.1]. The difference of this approximation is found to be within 1dB (Fig.4.1) [4.1]. The following approximation is carried out for $k \geq 2$ and $BER \leq 10^{-3}$.

$$BER_{M - \text{QAM}} \approx 0.2 \exp \left[\frac{-1.6 * SNR}{2^k - 1} \right] \quad (4.2)$$

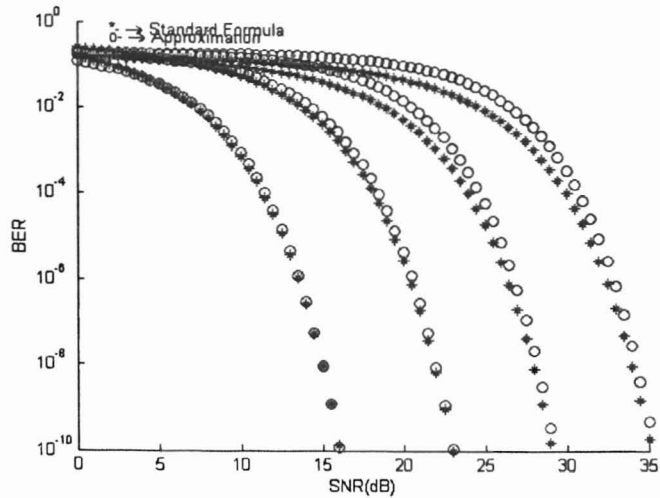


Fig.4.1. BER for M -QAM

Now, the BER approximation can be defined, where k is found from the above equation and compared with the Shannon capacity limit. The spectral efficiency is plotted (Fig.4.2) and compared for different BER requirements (10^{-3} and 10^{-6}). Taking logarithm on both sides of equation (4.2), we obtain the following derivations:

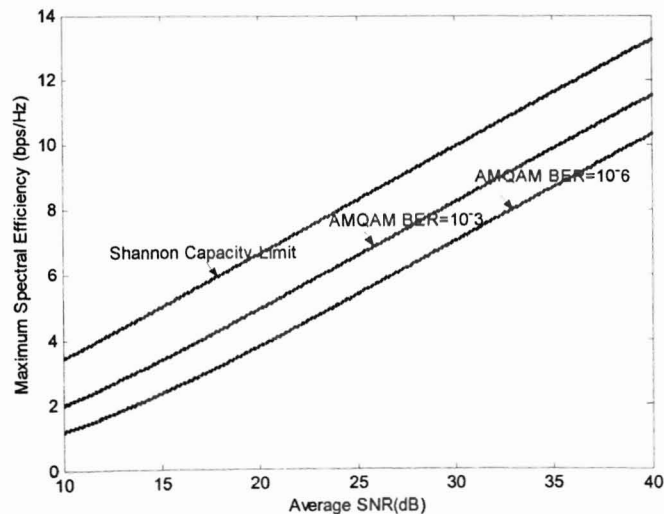


Fig.4.2. Maximum spectral efficiency for continuous rate adaptation.

$$\frac{BER_{MQAM}}{0.2} \approx \exp\left[\frac{-1.6 * SNR}{2^k - 1}\right]$$

$$\ln\left(\frac{BER_{MQAM}}{0.2}\right) = \ln\left(\exp\left[\frac{-1.6 * SNR}{2^k - 1}\right]\right)$$

$$\ln(5BER_{MQAM}) = \left[\frac{-1.6 * SNR}{2^k - 1}\right]$$

Based on the results we can see that

$$2^k - 1 = \left[\frac{-1.6 * SNR}{\ln(5BER_{MQAM})}\right]$$

$$2^k = 1 + \left[\frac{-1.6 * SNR}{\ln(5BER_{MQAM})}\right]$$

From the above equation we obtain,

$$k = \log_2\left(1 + \left[\frac{-1.6 * SNR}{\ln(5BER_{MQAM})}\right]\right) \quad (4.3)$$

Based on equation (4.3) the spectral efficiency is plotted out in fig.4.2. It is evident from the three curves that the BER performance is achieved at the expense of spectral efficiency, ie., to achieve a BER of 10^{-6} the spectral efficiency has to be much lower (about 1.5bps/Hz) compared to the BER of 10^{-3} requirements, at a fixed SNR.

The approximation of the bit-error-rate for different channel conditions γ can be obtained from equation (4.4). The coefficients $c_1 = 0.2, c_2 = -1.6, c_3 = 1, c_4 = 1$ [4.1] were substituted to provide general access to the equation (4.4).

$$BER(\gamma) \approx c_1 \exp\left[\frac{-c_2 SNR(\gamma)}{2^{c_3 k(\gamma)} - c_4}\right] \quad (4.4)$$

Let \bar{S} denote the total transmitted signal power, then the instantaneous value of the received SNR can be represented by the equation $SNR(\gamma) = \gamma \frac{S(\gamma)}{\bar{S}}$, where $S(\gamma)$ is the instantaneous value of the power. Here $S(\gamma)$ is the adapted transmit power for received γ .

To obtain the instantaneous bit-error-rate equation, the average BER is equated to the instantaneous BER as given below: $\overline{BER} = BER(\gamma)$

$$\overline{BER} = BER(\gamma) \approx c_1 \exp \left[\frac{-c_2 SNR(\gamma)}{2^{c_3 k(\gamma)} - c_4} \right]$$

Taking natural logarithm of the above equation yields

$$\ln \frac{\overline{BER}}{c_1} \approx \left[\frac{-c_2 SNR(\gamma)}{2^{c_3 k(\gamma)} - c_4} \right],$$

which can be reorganized in the form of

$$2^{c_3 k(\gamma)} - c_4 \approx \left[\frac{-c_2 SNR(\gamma)}{\ln \frac{\overline{BER}}{c_1}} \right].$$

And correspondingly,

$$2^{c_3 k(\gamma)} \approx \left[\frac{-c_2 SNR(\gamma)}{\ln \frac{\overline{BER}}{c_1}} + c_4 \right]$$

$$c_3 k(\gamma) \approx \log_2 \left[\frac{-c_2 \overline{SNR}(\gamma)}{\ln \frac{BER}{c_1}} + c_4 \right]$$

$$k(\gamma) \approx \frac{\log_2 \left[\frac{-c_2 \overline{SNR}(\gamma)}{\ln \frac{BER}{c_1}} + c_4 \right]}{c_3} . \quad (4.5)$$

Number of modulation bits ($k(\gamma)$) for M -QAM: The continuous levels of modulation and the discrete levels used in the adaptive rate system are shown in the following figures Fig.4.3, 4.4, 4.5, 4.6. No transmission occurs when the channel condition is below the desired SNR level. In this case, no modulation bit is employed. In Figs. 4.4-4.6, the adaptation threshold value is assumed to be 5 dB for Rayleigh channel for a BER of 10^{-3} . Based on the continuous level, the adaptation system takes infinite continuous switching levels, whereas the discrete adaptation system takes finite switching levels based on the target BER conditions for the data system. For the case shown below, the switching levels in case of discrete adaptation comprise of $k(\gamma) = 0, 2, 4, 6, 8, 10,$ and 12 . The number of degrees of freedom is assumed based on implementation considerations.

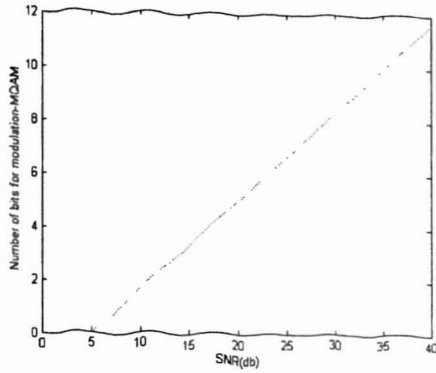


Fig.4.3. Continuous rate average BER.

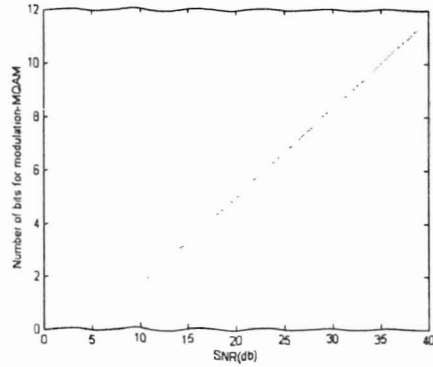


Fig.4.4. Continuous rate instantaneous BER.

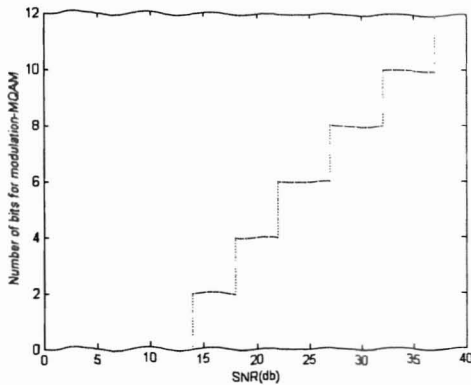


Fig.4.5. Discrete rate average BER.

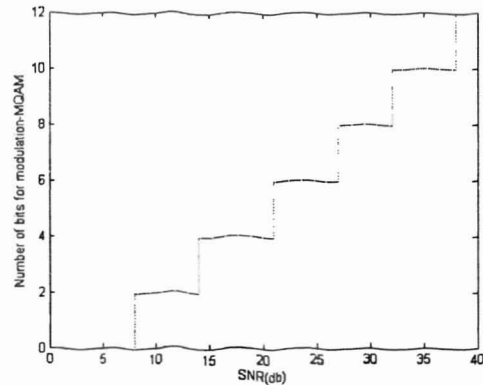


Fig.4.6. Discrete rate instantaneous BER.

4.2. Optimal Power Adaptation:

1) **Continuous rate adaptation:** Since there are two variables to be optimized- (transmitter power and adaptation rate), we introduce two Lagrange variables – (λ_1 and λ_2). The Lagrange equation for the instantaneous BER is given in terms of power and rate by,

$$J(S(\gamma), k(\gamma)) = \int_0^{\infty} k(\gamma) p(\gamma) d\gamma + \lambda_1 \int_0^{\infty} BER(\gamma) k(\gamma) p(\gamma) d\gamma - \overline{BER} \int_0^{\infty} k(\gamma) p(\gamma) d\gamma + \lambda_2 \int_0^{\infty} S(\gamma) p(\gamma) d\gamma - \overline{S}$$

Since for instantaneous BER, $BER(\gamma) = \overline{BER}$, the above equation can be reduced to one

Lagrange variable,

$$J(S(\gamma)) = \int_0^{\infty} \frac{\log_2 \left[\frac{-c_2 SNR(\gamma)}{\ln \frac{BER}{c_1}} + c_4 \right]}{c_3} p(\gamma) d\gamma + \lambda \int_0^{\infty} S(\gamma) p(\gamma) d\gamma - \overline{S}$$

$$SNR(\gamma) = \gamma \frac{S(\gamma)}{\overline{S}}$$

Performing optimal power condition, $\frac{\partial J}{\partial S(\gamma)} = 0$ for $S(\gamma) \geq 0, k(\gamma) \geq 0$, the equation for the

power becomes

$$\frac{S(\gamma)}{\overline{S}} = -\frac{1}{c_3 (\ln 2) \lambda \overline{S}} - \frac{1}{\gamma K}$$

$$\frac{S(\gamma)}{\overline{S}} = \frac{1}{\gamma_0 K} - \frac{1}{\gamma K}, \quad (4.6)$$

where K gives the power loss when a non-adaptive QAM is used for modulation. It is

given by the equation,

$$K = -\frac{c_2}{c_4 \ln \left(\frac{BER}{c_1} \right)}.$$

The power adaptation equation is a water filling equation, which means that more power

is used when the channel quality is good. The cutoff fade depth is given by γ_0 below

which $S(\gamma) = 0$. The above equation is plotted as shown in the figure 4.7.

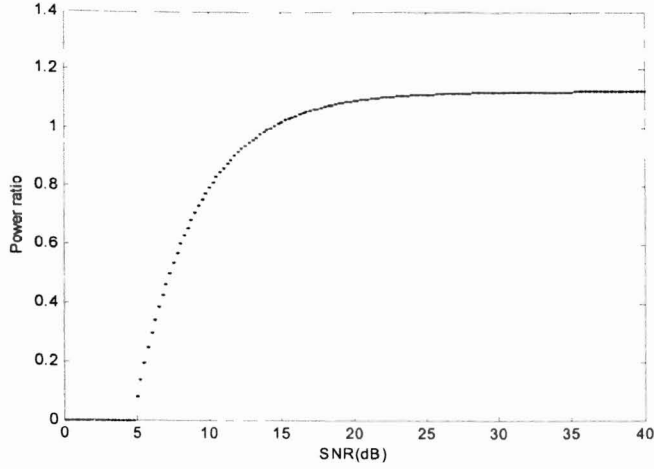


Fig.4.7. $\frac{S(\gamma)}{\bar{S}}$ for MQAM

In adaptive OFDM (AOFDM) systems, depending on the channel conditions the modulation parameters are varied. The channel threshold SNR value above which transmission takes place is given by γ_0 . For the conditions above, $S(\gamma) = 0$ for $\gamma < \gamma_0$. The term $J(\gamma_1, \gamma_2, \dots, \gamma_N, S(\gamma))$ is the Langrange multiplier equation for the variables, adaptive rate and adaptive power. It is given by

$$J(\gamma_1, \gamma_2, \dots, \gamma_N, S(\gamma)) = \sum_{0 \leq i \leq N-1} k_i \int_{\gamma_i}^{\gamma_{i+1}} p(\gamma) d\gamma + \lambda_1 \left[\sum_{0 \leq i \leq N-1} k_i \int_{\gamma_i}^{\gamma_{i+1}} (BER(\gamma) - \overline{BER}) p(\gamma) d\gamma \right] + \lambda_2 \left[\int_{\gamma_0}^{\infty} S(\gamma) p(\gamma) d\gamma - \bar{S} \right]$$

The optimal power and rate adaptations are obtained from solving the following conditions:

$$\frac{\partial J(\gamma_1, \gamma_2, \dots, \gamma_N, S(\gamma))}{\partial S(\gamma)} = \frac{\partial}{\partial S(\gamma)} \sum_{0 \leq i \leq N-1} k_i \int_{\gamma_i}^{\gamma_{i+1}} p(\gamma) d\gamma + \lambda_1 \frac{\partial}{\partial S(\gamma)} \left[\sum_{0 \leq i \leq N-1} k_i \int_{\gamma_i}^{\gamma_{i+1}} (BER(\gamma) - \overline{BER}) p(\gamma) d\gamma \right]$$

$$\begin{aligned}
& + \lambda_2 \frac{\partial}{\partial S(\gamma)} \left[\int_{\gamma_0}^{\infty} S(\gamma) p(\gamma) d\gamma - \bar{S} \right] \\
= & 0 + \lambda_1 \left[\frac{\partial}{\partial S(\gamma)} \sum_{0 \leq i \leq N-1} k_i \int_{\gamma_i}^{\gamma_{i+1}} (BER(\gamma) p(\gamma) d\gamma - 0) \right] + \lambda_2 \left[\int_{\gamma_0}^{\infty} \frac{\partial}{\partial S(\gamma)} S(\gamma) p(\gamma) d\gamma - 0 \right] \\
& = 0 + \lambda_1 k_i \frac{\partial BER(\gamma)}{\partial S(\gamma)} + \lambda_2 .
\end{aligned}$$

In summary, we obtain,

$$\frac{\partial BER(\gamma)}{\partial S(\gamma)} = \frac{-\lambda_2}{\lambda_1 k_i} . \quad (4.7)$$

Substituting $BER_{MQAM} \approx 0.2 \exp \left[\frac{-1.6 * SNR}{2^{k_i} - 1} \right]$ in the equation (4.7), we get,

$$\frac{\partial}{\partial S(\gamma)} \left[0.2 \exp \left[\frac{-1.6 * \gamma \frac{S_i(\gamma)}{\bar{S}}}{2^{k_i} - 1} \right] \right] = \frac{-\lambda_2}{\lambda_1 k_i} . \quad (4.8)$$

To simplify (4.8), we substitute $2^{k_i} - 1 = f(k_i)$ in which we obtain,

$$\begin{aligned}
& \frac{-1.6 * \frac{\gamma}{\bar{S}}}{f(k_i)} \left[0.2 \exp \left[\frac{-1.6 * \gamma \frac{S_i(\gamma)}{\bar{S}}}{f(k_i)} \right] \right] = \frac{-\lambda_2}{\lambda_1 k_i} \\
& \left[\exp \left[\frac{-1.6 * \gamma \frac{S_i(\gamma)}{\bar{S}}}{f(k_i)} \right] \right] = \frac{\lambda_2 f(k_i) \bar{S}}{\lambda_1 * 0.32 * k_i \gamma} .
\end{aligned}$$

Taking a logarithm on both sides we obtain,

$$\frac{-1.6 * \gamma \frac{S_i(\gamma)}{\bar{S}}}{f(k_i)} = \ln \left[\frac{\lambda f(k_i)}{3.2 * k_i \gamma} \right]$$

$$\frac{S_i(\gamma)}{\bar{S}} = \ln \left[\frac{\lambda f(k_i) \bar{S}}{-3.2 * k_i \gamma} \right] \frac{f(k_i)}{-1.6 * \gamma} \quad (4.9)$$

2) Discrete Rate, Instantaneous BER: In case of discrete rate analysis, k_i takes discrete values for the regions defined by $[\gamma_i, \gamma_{i+1})$. These rate region boundaries are determined by the average power and BER constraint. Assuming an instantaneous BER for analysis, we have, the average $\overline{BER} = BER(\gamma)$, which becomes

$$\overline{BER} \approx c_1 \exp \left[\frac{-c_2 SNR(\gamma)}{2^{c_3 k(\gamma)} - c_4} \right],$$

based on

$$SNR(\gamma) = \gamma \frac{S(\gamma)}{\bar{S}}.$$

Substituting, $2^{k_i} - 1 = f(k_i)$ we obtain,

$$\frac{S(\gamma)}{\bar{S}} = -\frac{f(k_i)}{c_2} \ln \left(\frac{\overline{BER}}{c_1} \right). \quad (4.10)$$

3) Constant rate, Instantaneous BER:

$$\frac{-1.6 * \gamma \frac{S_i(\gamma)}{\bar{S}}}{f(k_i)} = \ln \left[\frac{\lambda f(k_i)}{3.2 * k_i \gamma} \right]$$

$$\frac{S_i(\gamma)}{\bar{S}} = \ln \left[\frac{\lambda f(k_i) \bar{S}}{-3.2 * k_i \gamma} \right] \frac{f(k_i)}{-1.6 * \gamma} \quad (4.9)$$

2) Discrete Rate, Instantaneous BER: In case of discrete rate analysis, k_i takes discrete values for the regions defined by $[\gamma_i, \gamma_{i+1})$. These rate region boundaries are determined by the average power and BER constraint. Assuming an instantaneous BER for analysis, we have, the average $\overline{BER} = BER(\gamma)$, which becomes

$$\overline{BER} \approx c_1 \exp \left[\frac{-c_2 SNR(\gamma)}{2^{c_3 k(\gamma)} - c_4} \right],$$

based on

$$SNR(\gamma) = \gamma \frac{S(\gamma)}{\bar{S}}.$$

Substituting, $2^{k_i} - 1 = f(k_i)$ we obtain,

$$\frac{S(\gamma)}{\bar{S}} = -\frac{f(k_i)}{c_2} \ln \left(\frac{\overline{BER}}{c_1} \right). \quad (4.10)$$

3) Constant rate, Instantaneous BER:

The spectral efficiency of the modulation scheme is defined as the average data rate per unit bandwidth (R/B). Since the rate is kept constant, k can be taken outside the integration and hence the equation becomes,

$$\frac{R}{B} = k \int_{\gamma_0}^{\infty} p(\gamma) d\gamma ,$$

which we apply

$$2^k - 1 = f(k) ,$$

and obtain

$$\frac{S(\gamma)}{\bar{S}} = \ln \left[\frac{\lambda f(k) \bar{S}}{c_1 c_2 * k \gamma} \right] - \frac{f(k)}{c_2 * \gamma} . \quad (4.11)$$

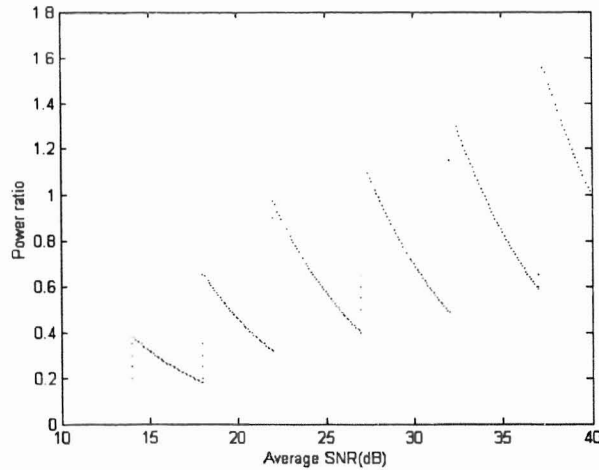


Fig.4.8. Power ratio for Adaptive M -QAM systems.

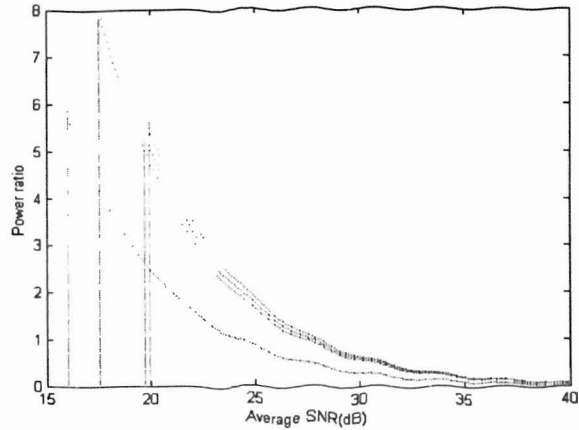


Fig.4.9. Power ratio for constant rate, adaptive power systems.

4.3. Spectral Efficiency of Adaptive M -QAM for discrete rate adaptation:

1) Discrete Rate and Average Bit Error Rate: In case of discrete rate adaptive modulation, k takes discrete values within $0 \leq k \leq N-1$. From the equation of spectral efficiency,

$$SpectralEfficiency = \log_2 \left(1 + \left[\frac{-1.6 * SNR}{\ln(5BER_{M-QAM})} \right]_M \right) \quad M \text{ represents the number of signal}$$

constellations given by 2^k and the discrete boundaries of M are considered to be within 6 regions given by $M = 0, 2, 4, 16, 64,$ and 256 .

With the discrete constellation sizes at appropriate region boundaries the suboptimal spectral efficiency is selected as shown in the figure fig.4.10. It is found from the graphs below that the continuous rate modulation yields the highest spectral efficiency while the discrete rate system also yields a close efficient spectral performance.

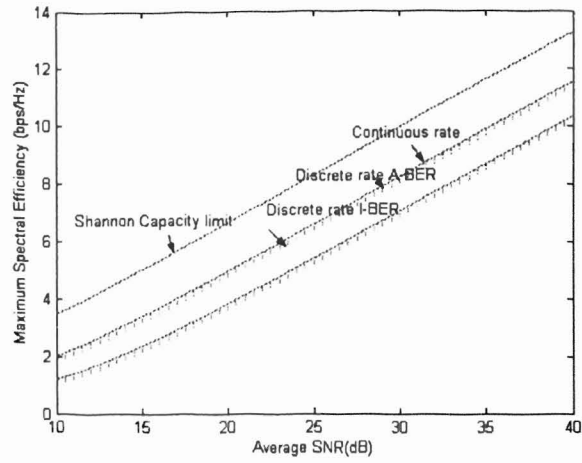


Fig.4.10. Spectral Efficiency for Variable rate, Variable power M -QAM systems.

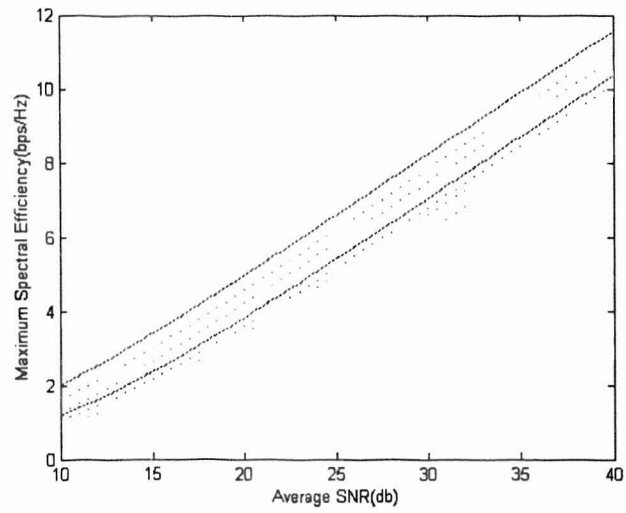


Fig.4.11. Spectral Efficiency for M -QAM systems with constant transmit power.

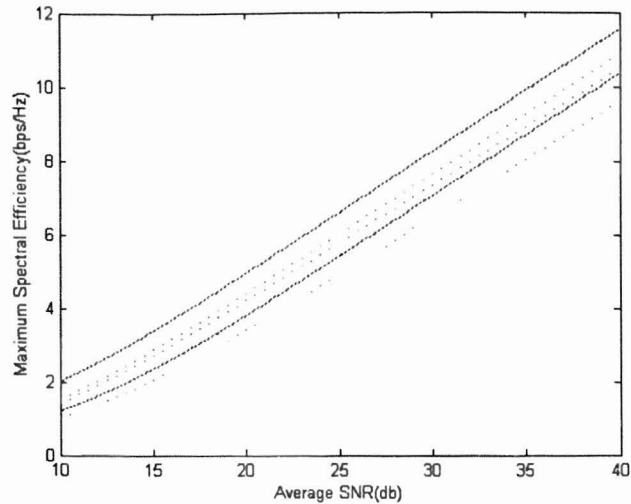


Fig.4.12. Spectral Efficiency for constant rate M -QAM systems.

Fig.4.10. shows the spectral efficiency achieved on a variable rate, variable power adaptation system for continuous and discrete systems.

4.4. Constant power, Adaptive Rate and Constant Rate, Adaptive Power Systems

Constant Power, Instantaneous BER: The same analysis is also carried out for a single adaptation system – for both the variable rate and the variable power adaptive system. Fig.4.2 and fig.4.3 gives the resulting spectral efficiency achieved with the single variable adaptive system. With the restriction of either constant power or rate with or without thresholds, the adaptive system is further analyzed for the possible loss of spectral efficiency.

Constant Power Instantaneous BER: From (4.2),

$$k(\gamma) \approx \frac{\log_2 \left[\frac{-c_2 SNR(\gamma) + c_4}{\ln \frac{BER}{c_1}} \right]}{c_3} .$$

Substituting, $SNR(\gamma) = \gamma \frac{S(\gamma)}{S}$, we obtain,

$$k(\gamma) \approx \frac{\log_2 \left[\frac{-c_2 \gamma \frac{S(\gamma)}{S} + c_4}{\ln \frac{BER}{c_1}} \right]}{c_3} .$$

The Lagrange equation for the instantaneous BER is given by,

$$J(S(\gamma), k(\gamma)) = \int_0^{\infty} k(\gamma) p(\gamma) d\gamma + \lambda_1 \int_0^{\infty} BER(\gamma) k(\gamma) p(\gamma) d\gamma - \overline{BER} \int_0^{\infty} k(\gamma) p(\gamma) d\gamma + \lambda_2 \int_0^{\infty} S(\gamma) p(\gamma) d\gamma - \overline{S} .$$

Since for the instantaneous BER, $BER(\gamma) = \overline{BER}$, the above equation is reduced to one

Lagrange variable given by

$$J(k(\gamma)) = \int_0^{\infty} k(\gamma) p(\gamma) d\gamma + \lambda \int_0^{\infty} S(\gamma) p(\gamma) d\gamma - \overline{S} .$$

This is possible due to the constant power condition. The Lagrange equation with two variables of adaptive rate and adaptive power can be reduced to a single variable for adaptive rate only.

Differentiating w.r.t. rate and given a constant power of $S(\gamma) = S$, we have

$$\frac{S}{S} = \frac{1}{\int_{\gamma_0}^{\infty} p(\gamma) d\gamma}$$

Therefore,

$$k(\gamma) \approx \frac{\log_2 \left[\frac{-c_2 \gamma \frac{1}{\int_{\gamma_0}^{\infty} p(\gamma) d\gamma}}{\ln \frac{BER}{c_1}} + c_4 \right]}{c_3}$$

The spectral efficiency for a constant rate system can be given by

$$\begin{aligned} \frac{R}{B} &= \int_{\gamma_0}^{\infty} k(\gamma) p(\gamma) d\gamma \\ &= \int_{\gamma_0}^{\infty} \frac{\log_2 \left[\frac{-c_2 \gamma \frac{1}{\int_{\gamma_0}^{\infty} p(\gamma) d\gamma}}{\ln \frac{BER}{c_1}} + c_4 \right]}{c_3} p(\gamma) d\gamma \end{aligned}$$

With $p(\gamma)$ as an exponential distribution function and with a zero threshold value, the above equation can be reduced to

$$\frac{R}{B} = \int_{\gamma_0}^{\infty} \frac{\log_2 \left[\frac{-c_2 \gamma}{\ln \frac{BER}{c_1}} + c_4 \right]}{c_3} p(\gamma) d\gamma \quad (4.12)$$

The results of equation (4.12) is plotted in Fig.4.11.

4.5. BER performance results of the continuous and discrete rate adaptation systems

To obtain the performance of the variable-rate and variable-power systems, for the continuous adaptive rate case we apply equations (4.3) and (4.2) to obtain Fig.4.13, and for discrete k adaptive case we apply (4.3) with discrete levels into the Matlab program provided in Appendix A (program 8.m) to obtain the results in Fig.4.14.

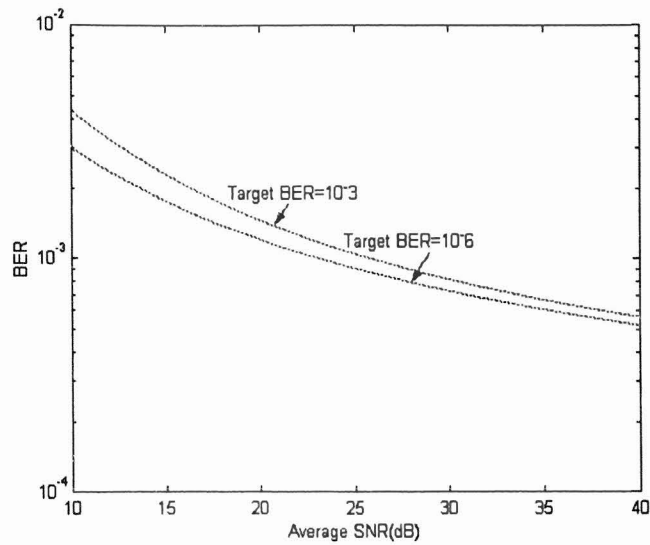


Fig.4.13. BER for continuous rate adaptive modulation.

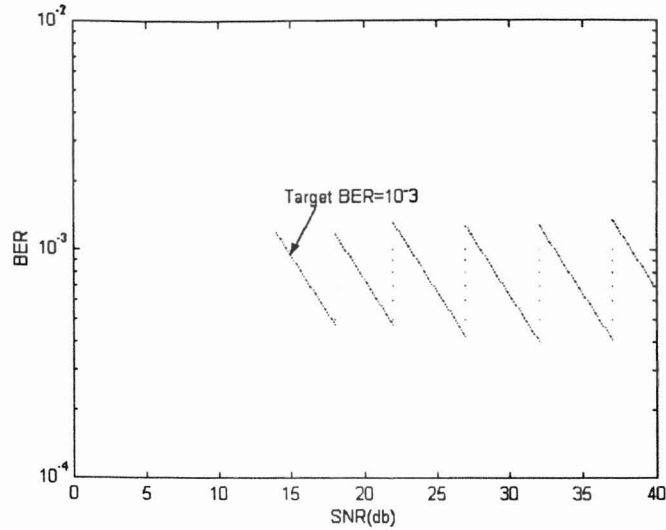


Fig.4.14. BER for discrete rate adaptive modulation.

4.6. Observations

The numerical results plotted in this chapter are for a BER of 10^{-3} and 10^{-6} Rayleigh fading results and taking into consideration only a flat fading distribution [4.1]. The BER approximations and the Lagrange expressions are carried out for single-carrier modulation. The spectral efficiency figures shown in Fig.4.2, Fig.4.10, and Fig.4.11 show that there is not much of a difference in the spectral efficiency obtained for the continuous rate and discrete rate adaptation technologies. This means that discrete rate adaptation can be processed without much of a spectral loss. The optimal BER adaptation curve is shown in Fig.4.13 and Fig.4.14 for the constrained average BER of 10^{-3} .

This system model applying adaptive rate and adaptive power control has been applied for OFDM modulation in this chapter. Further, in the following chapter, the numerical analysis is extended to also include lognormal fading systems (shadowing effects) and also investigate the system features of macroscopic diversity combining.

CHAPTER 5

ADAPTIVE MODULATION FOR OFDM SYSTEM AND MACROSCOPIC DIVERSITY TECHNIQUES

In this chapter the adaptive rate and adaptive power modulation, and BER approximation model (by Chung and Goldsmith [4.1]) is combined with an OFDM system. The signaling and detection techniques and their probability of false alarm are also calculated. In the second part of this chapter, the macroscopic diversity techniques are combined with the developed adaptive OFDM.

In [5.7], Steele and Webb introduced the adaptive M -QAM for burst-by-burst adaptation for QAM modulation. In this research, the adaptive rate and adaptive power M -QAM multicarrier modulation technique is considered on an OFDM-TDMA channel for mobile communication systems. The mobile channel suffers from flat fading. The OFDM system with the help of adaptive modulation reduces the BER and improves the performance with the efficient use of the bandwidth. The investigation is further extended to the analysis of the signaling and detection of the modulation technique using pilot carriers.

5.1. Adaptive OFDM

Since fixed OFDM transmission systems are not well suited for varying channel conditions, adaptive OFDM modems are investigated as a mean to improve the performance. OFDM transmitter parameter adaptation is an action of the transmitter in

response to time varying channel conditions. It is only suitable for duplex communication because the transmission parameter depends on some form of signaling and channel estimation. To improve the performance of an OFDM system, subcarrier modulation modes can be adapted to the channel conditions. For subcarriers exhibiting low SNR levels, low modulation levels are used, whereas the subcarriers with a high SNR can be set for a higher multilevel modulation scheme.

The thesis is based on an OFDM system with N data symbols S_n , where n ranges from 0 to $N-1$. These symbols are multiplexed over N subcarriers. The time-domain samples s_n are generated by the inverse fast Fourier transform (IFFT) and transmitted over the channel after the cyclic prefix is inserted. On the receiver side, the OFDM time-domain samples are subject to the removal of cyclic extension followed by the fast Fourier transform (FFT) to receive the data symbols R_n . The received data symbols can be expressed as [5.1]

$$R_n = S_n \cdot H_n + n_n \quad (5.1)$$

where n_n is the AWGN sample.

The following procedures are to be followed for an adaptive OFDM system.

a) Channel Quality Estimation: In order to execute the adaptive modulation techniques, the transmitter and receiver should have knowledge of the channel conditions. There are two types of channel quality estimation known as *open-loop adaptation* and *closed-loop adaptation*. In case of *open-loop adaptation* (a TDD system),

where the channel is duplex, each station can estimate the quality of the channel by the use of received OFDM symbols. In case of the closed-loop adaptation (an FDD system) where the channel is not reciprocal, the receiver explicitly invokes the remote transmitter as to which modem mode to adapt to for the next active time slot. In our analysis, the system assumes *open-loop adaptation*.

b) Determination of Modulation Parameters for the subcarriers: This is performed by the method described in section 5.2 below using pilot symbol detection.

5.2. Modulation Parameters in case of Adaptive Modulation of subcarriers

For a higher throughput, a higher proportion of low-quality OFDM subcarriers have to be used for the transmission of inherently vulnerable high-order modem modes, transmitting several bits per subcarrier. Many researchers have demonstrated adaptive subcarrier selection and the results show BER performance improvements ([5.1], [5.2], [5.3]).

There are various kinds of adaptivity that can be applied to an OFDM system. Two types of systems are looked into in the current research. The first one is based on subcarrier-by-subcarrier basis and the second type is the subband adaptive modulation. In this thesis, to reduce the system complexity, the OFDM modulation is not applied on a subcarrier-to-subcarrier basis but instead it is divided into subbands consisting of a set of subcarriers and this subband is assigned a single modulation level according to the channel conditions.

The modulation of the subcarriers is allocated block by block. Consider an N -subcarrier (say 512 subcarriers) OFDM system with K number of users in a WLAN

system with a carrier frequency of 60 GHz. Consider the different types of modulations applied to the system as M_n where n is 0, 1, 2, 3, 4, 5, and 6 depending on the various modulation schemes as: no modulation, BPSK, QPSK, 8-PSK, 16-QAM, 64-QAM.

The average modulation level M is given by,

$$\frac{1}{N_b} \sum_{n=0}^{N_b-1} M_n = M$$

This section discusses two issues. First, Keller and Hanzo's adaptive algorithm [5.3] is studied and second, based on [4.1], adaptive rate and adaptive power OFDM system BER performance results are compared with the results from the model applied in [5.3].

Choice of the Modulation Scheme: There are three schemes suggested by the researchers for the selection of the modulation scheme [5.3]. In this thesis, we analyze the performance of the Fixed Threshold Adaptation Algorithm.

Fixed Threshold Adaptation Algorithm: This adaptation algorithm is assumed for a constant instantaneous SNR over all of the symbols in a subband. If the subband is larger than the coherence bandwidth, then this algorithm will not hold good leading to a penalty of throughput due to the frequency selective channel with the channel quality varying for different subcarriers. When the SNR of the switching level l_n falls in the range given by the table 5.1, then the corresponding modulation level M_n is selected as the modulation level for that subband.

Switching Levels:

0 dB to 3.31 dB	3.31 dB to 6.8 dB	6.8 dB to 11 dB	> 11 dB
No modulation	BPSK, M=2, k=1	QPSK, M=4, k=2	16-QAM, M=16, k=4

Table 5.1. Adaptive Modulation Look-Up Table

Proposed system:

a) The following BER approximation system was used in [4.1] for an M -QAM system, and in this chapter it has been applied with a variable rate and variable power AOFDM system applying Hanzo's BER estimator adaptation algorithm. A Performance analysis of the two systems in a Rayleigh fading channel is given in Fig.5.1.

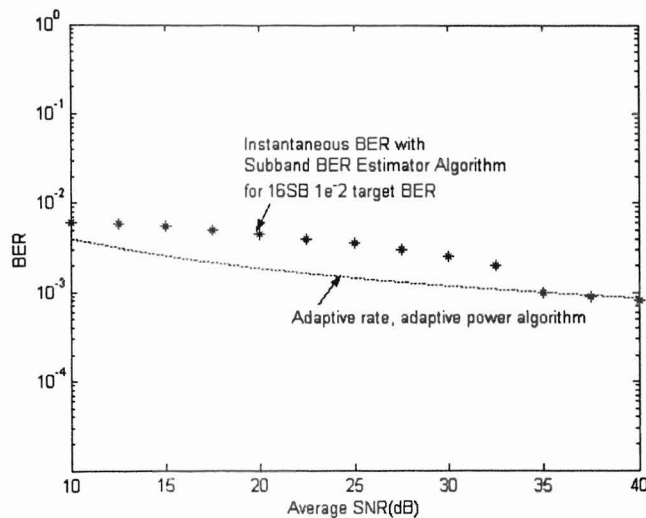


Fig.5.1. BER performance of the proposed OFDM system.

Fig.5.1. resulted by taking into account the channel conditions and its corresponding SNR of [4.3].

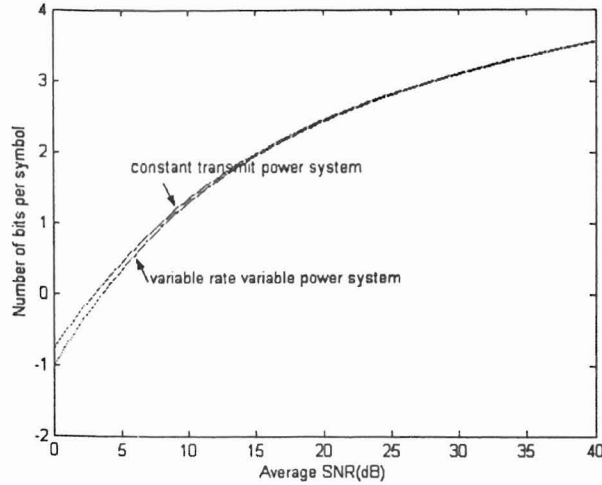


Fig.5.2. Throughput performance of the proposed OFDM system.

From Fig.5.1, it is found that the BER performance for the proposed system is almost a steady BER performance curve compared to the rapidly varying BER performance of a constant transmitter power system. Fig.5.2. shows the throughput efficiency of the two systems. Based on the results of Fig.5.2., it is evident that there is not much of a tradeoff in throughput between the two systems for a given BER of 10^{-3} .

5.3. Signaling and Blind Detection

The receiver needs to have knowledge of the modulation scheme used for the different subbands. This is achieved by the use of Pilot Symbol Aided Modulation techniques.

a) Signaling: The simplest way of signaling is just replacing one data symbol by a signaling symbol of a known modulation. Coherent phase detection is performed at the receiver and an error free detection is assumed.

While transmitting data on the channel, one of the data symbols are replaced by M -PSK symbol, where M is the number of the modulation scheme. When employing one symbol for signaling, the signaling error probability is given by the above equation. In [5.3], the signaling symbol is QPSK modulated. The detection error probability when using one symbol for detection is given by

$$p_s(\gamma) = 1 - \left(1 - \frac{1}{2} \operatorname{erfc}\left(\sqrt{\frac{\gamma}{2}}\right)\right)^2 \quad (5.2)$$

where $p_s(\gamma)$ gives the detection error probability function and γ is the average channel SNR. The signaling error probability in case of N_s signaling symbols can be expressed as [5.3]

$$p_s(\gamma) = 1 - \left(1 - \frac{1}{2} \operatorname{erfc}\left(\sqrt{\frac{\gamma N_s}{2}}\right)\right)^2. \quad (5.3)$$

The results of equation (5.3) is shown in Fig.5.3.

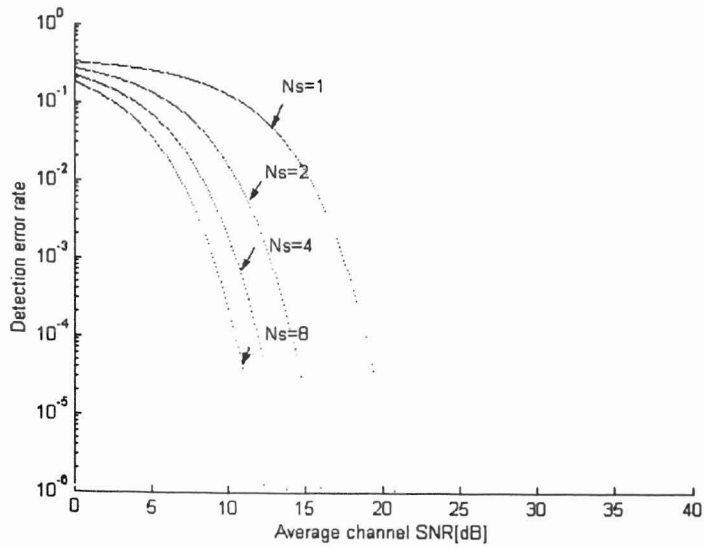


Fig.5.3. Probability of erroneous detection of existing system.

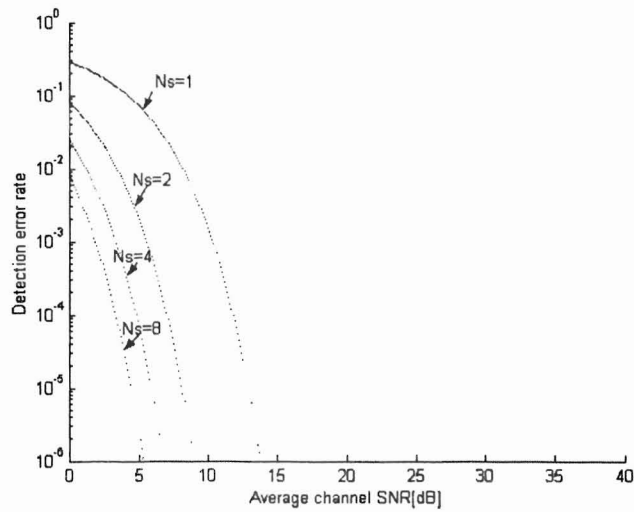


Fig.5.4. Probability of erroneous detection of proposed system.

Applying the BER approximation from [4.1], we get

$$BER_{M-QAM} \approx 0.2 \exp \left[\frac{-1.6 * SNR}{2^k - 1} \right],$$

$$p_s(\gamma) = 1 - (1 - BER_{M-QAM})^2. \quad (5.4)$$

The results of the equation (5.4) is plotted in Fig.5.4. From Fig.5.3 and Fig.5.4, it is evident that the The proposed adaptive system of using the BER approximation given below yields a lower detection error compared to the existing system.

5.4. Macroscopic diversity

Diversity is known to be an effective method of reducing the deleterious effects of the fading in radio channels. Diversity techniques can be used to reduce the signal variability. The concept behind space diversity is relatively simple. If one signal undergoes a deep fade at a particular point of time, another independent signal component detected at a distance location may have a strong signal. This technique when combined with adaptive modulation system could yield an improved BER performance.

There are various types of diversity used in communication systems operating over fading channels. They are: Space Diversity, Frequency Diversity, Time Diversity, Polarization Diversity, and Multipath Diversity.

Whatever the diversity technique employed is, the receiver has to process the diversity signals obtained in a fashion that maximizes the power efficiency of the system. There are several possible diversity reception methods employed in communication receivers. The most common techniques are: Selection Diversity, Equal Gain Combining (EGC), and Maximal Ratio Combining (MRC).

The aim of this section is to study the improvement achieved by the use of Macroscopic Selection Diversity on adaptive rate and adaptive power systems (modeled in Chapter 4) thus reducing the overall BER of the system. Space diversity is achieved by

placing different base stations separated large enough so that the resultant components at each base station (i.e., the fast (Rayleigh) and slow (lognormal) fading components) are independent. Macroscopic diversity is then performed on the mean of each system and the BER performance is analyzed. In this section, the probability of BER of non-macroscopic and macroscopic diversity systems (analysis is done with three base station for one mobile system) are compared and the results are plotted using Matlab via Monte Carlo simulations.

a) Radio Channel model

The channel model considered in this chapter is a mobile radio channel model. The radio channel is characterized by multipath propagation of the signal due to diffraction and scattering from buildings. The received signal is characterized by fast fading, superimposed by the slow fading due to the shadowing effects. The fast fading envelope is modeled as a Rayleigh distribution while the slow fading is characterized as a lognormal component with a standard deviation in the range of 9-12dB.

b) Probability of non-macroscopic diversity techniques

The PDF of the lognormal density function including the multipath and shadowing effects is given using the approximation method of [5.8], which results in the form of

$$p(\gamma) = \frac{10}{\gamma\sigma \log_e 10\sqrt{2\pi}} \times \exp\left[-\frac{(10\log_{10} \gamma - m)^2}{2\sigma^2}\right] \quad (5.5)$$

with mean m and standard deviation σ .

The probability of bit error using adaptive rate and adaptive power M -QAM modulation is given by

$$P_{BER(M-QAM)} = 0.2 \exp\left[\frac{-1.6 * \gamma}{2^{k(\gamma)} - 1}\right].$$

The BER approximation of the lognormal and Rayleigh fading channel is implemented by applying the BER equation from [4.1] and integrating over the PDF distribution given in equation (5.5), which results in

$$P_{m-BER(M-QAM)} = \int_0^{\infty} P_{BER(M-QAM)}(\gamma) p(\gamma) d\gamma.$$

$$\frac{BER_{M-QAM}}{0.2} \approx \exp\left[\frac{-1.6 * \gamma}{2^{k(\gamma)} - 1}\right]$$

$$\ln\left(\frac{BER_{M-QAM}}{0.2}\right) = \ln\left(\exp\left[\frac{-1.6 * \gamma}{2^{k(\gamma)} - 1}\right]\right)$$

$$\ln\left(5BER_{M-QAM}\right) = \left[\frac{-1.6 * \gamma}{2^{k(\gamma)} - 1}\right]$$

$$2^{k(\gamma)} - 1 = \left[\frac{-1.6 * \gamma}{\ln\left(5BER_{M-QAM}\right)}\right]$$

$$2^{k(\gamma)} = 1 + \left[\frac{-1.6 * \gamma}{\ln\left(5BER_{M-QAM}\right)}\right]$$

(5.6)

The results of equation (5.6) are plotted out in Fig.5.5.

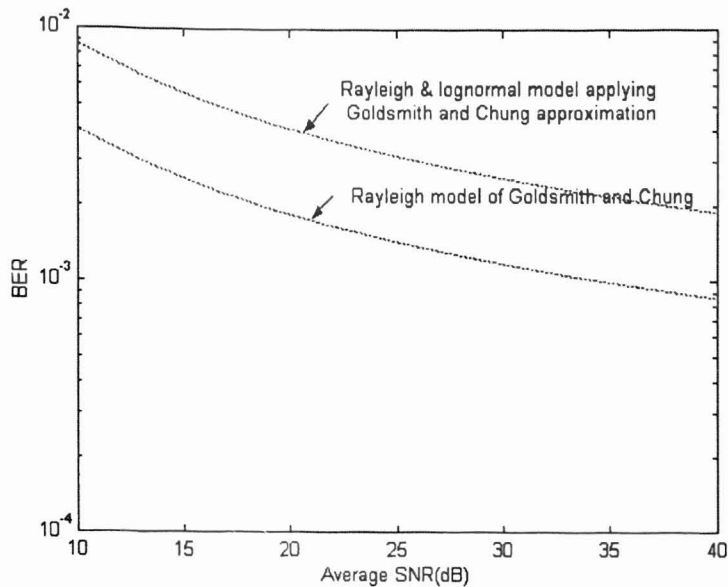


Fig.5.5. BER performance graph.

The effect of the lognormal shadowing is included with the adaptive rate and adaptive power BER approximation [5.8] for the required BER of 10^{-3} . Based on the Fig.5.5, it can be clearly observed that there is a large BER loss in case where shadowing effects are included in the radio channel model.

The following section proposes macroscopic diversity combining system that will be applied with the adaptive OFDM system to reduce this degradation in the BER performance due to the shadowing effects.

c) Probability of m -branch macroscopic diversity techniques

Assume 3 base stations each separated from the mobile station at equal distance. In this case, the mobile station is assumed to receive the same strength of signals. Therefore, the

assumption applied in the simulation is $m_1 = m_2 = m_3 = 0\text{dB}$ and $\sigma_1 = \sigma_2 = \sigma_3 = 9\text{dB}$ for the three base station signals.

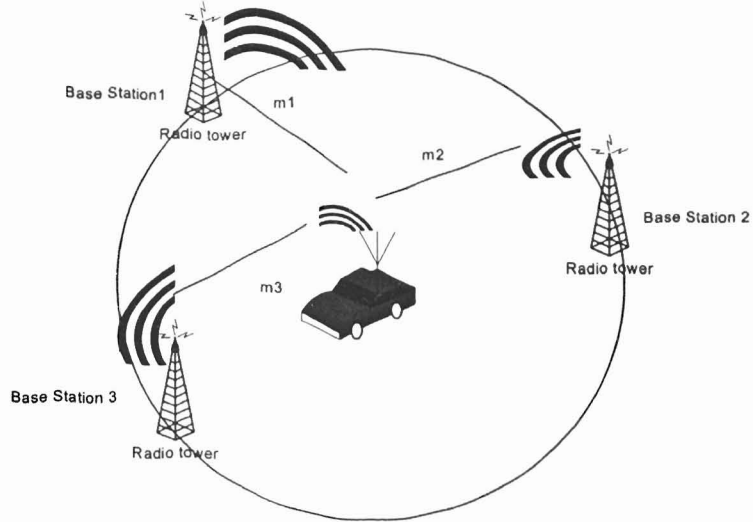


Fig.5.6. Three base stations at equal distance.

The probability of bit error of the m -branch macroscopic diversity system is given by [5.8]

$$P_{m-BER(M-QAM)} = \int_0^{\infty} P_{BER(M-QAM)}(\gamma) p_m(\gamma) d\gamma \quad (5.7)$$

where $P_{BER(M-QAM)} = 0.2 \exp\left[\frac{-1.6 * \gamma}{2^{k(\gamma)} - 1}\right]$ is used from [4.1] and $k(\gamma)$ is given by

$$k(\gamma) = \log_2 \left(1 + \left[\frac{-1.6 * SNR}{\ln(5BER_{M-QAM})} \right] \right) \quad (5.8)$$

The PDF of the m branch macroscopic diversity system is given by the following approximation,

$$P_m(\gamma) = \frac{10m}{\gamma\sigma_i \log_e 10\sqrt{2\pi}} \times \exp\left[-\frac{(10\log_{10}\gamma - m_i)^2}{2\sigma_i^2}\right] \times \left[P\left(\frac{10\log_{10}\gamma - m_i}{\sigma_i}\right)\right]^{m-1}, \quad (5.9)$$

where $P\left(\frac{10\log_{10}\gamma - m_i}{\sigma_i}\right)$ is the cumulative normal distribution function with mean

$m_i = m_1 = m_2 = m_3 = 0\text{dB}$ and standard deviation $\sigma_i = \sigma_1 = \sigma_2 = \sigma_3 = 9\text{dB}$.

Substituting equations (5.8) and (5.9) in (5.7) and integrating the resulting equation via Monte Carlo simulation, the final solution results in Fig.5.7.

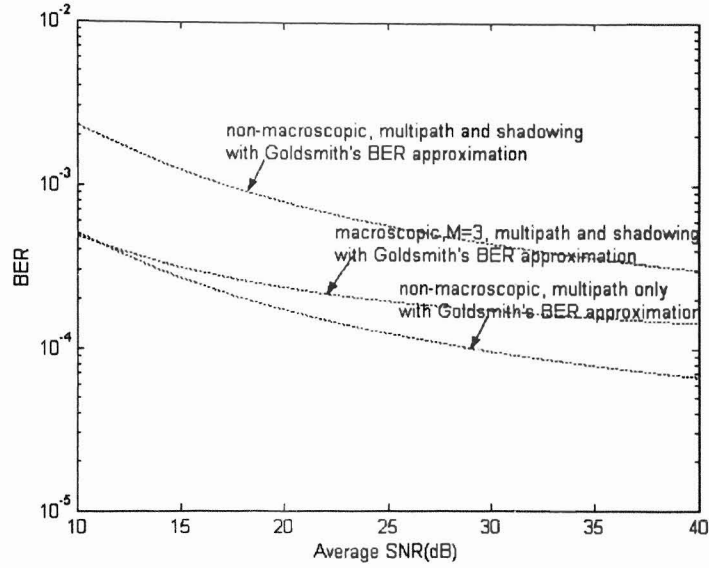


Fig.5.7. BER performance results in macroscopic diversity system.

Comparing Fig.5.5. and Fig.5.7, it is found that when multiple antennas are used (macroscopic technique) in a radio channel (with both multipath and shadowing), significant improvements in the BER performance can be obtained.

In most cases, the base stations may not be equally spaced from the mobile station. In this case, the signal received by the nearest base station is more likely to be stronger.

- a) Case (i): Let the mean of the received signal from first base station be m_1 , the second- m_2 and the third- m_3 . In the first case, the mobile station is assumed to be close to one base station compared to the other two stations. In this case, we have, $m_1 > m_2 = m_3$.

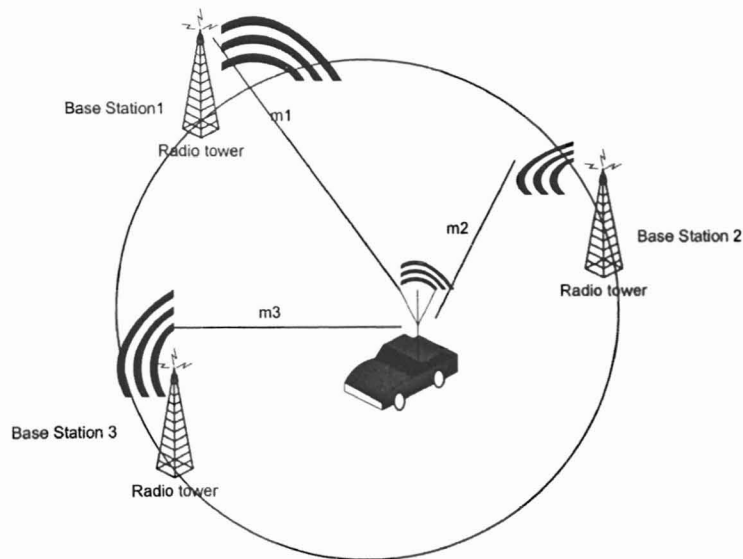


Fig.5.8. Three base stations at equal distances.

- b) Case (ii): Another possible case could be when the mobile station is closer to two of the base stations i.e., m_2 and m_3 than it is to the other one (m_1). In this case, we have, $m_2 = m_3 > m_1$ as the condition.

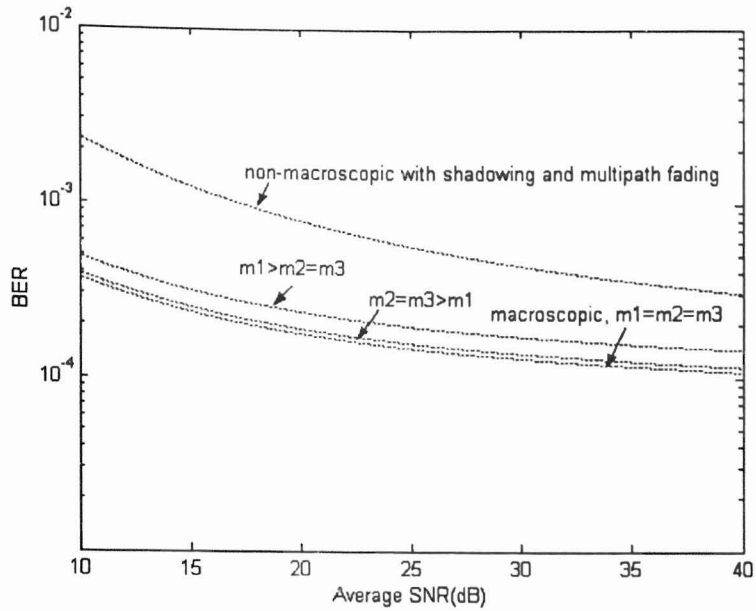


Fig.5.9. BER performance for unequal macroscopic diversity.

The performance of the M -branch macroscopic diversity technique is plotted in Fig.5.9. For a BER of 2×10^{-4} an improvement of around 20dB in SNR is achieved by using the 3-branch macrodiversity combining system. With the increase in the number of macrodiversity combining branches, the BER performance reaches an upper bound constant value.

CHAPTER 6

CONCLUSIONS & FUTURE RESEARCH

Two conclusions are derived from this research. First, based on the research in Chapters 3 and 4, adaptive rate and adaptive power control when applied to OFDM systems yields a better BER performance with no reduction in the throughput of the system (Fig.5.1, 5.2, 5.3, 5.4). Secondly, by applying adaptive rate and power control the signaling and detection error rate is significantly reduced compared to the conventional system with a smaller number of symbols used for signaling.

The deleterious effects of multipath propagation and shadowing are dominant terms that are used to characterize mobile radio channels. The fast fading term is approximated using a Rayleigh fading distribution. In this thesis, the fast fading component is reduced by using the adaptive rate and adaptive power modulation incorporated applying the methods proposed in [4.1]. Slow fading follows a lognormal distribution. This thesis considers both Rayleigh and log-normal fading in mobile channels and attempts to provide a solution of using adaptive modulation with macroscopic diversity. The macroscopic diversity model proposed by Turkmani [5.8] is applied to the OFDM system to reduce the probability of bit error rate (BER). This is made possible by approximating a composite Rayleigh plus lognormal distribution by a simplified lognormal distribution (Fig.5.5, 5.6, and 5.7). The performance of the

macroscopic diversity systems with equal distant base stations provided a significant SNR gain for the BER ranges of 10^{-3} and 10^{-6} .

With the Monte Carlo integration and matlab simulation, the following two main observations are reached in this thesis. With the application of OFDM adaptive rate and adaptive power control, for a constraint BER of 1×10^{-3} , a gain of 25 dB in SNR (Fig.5.1) is achieved without coding for a Rayleigh fading system. Further, for a particular SNR value (say 25 dB in Fig.5.4), the BER approximation used for signal detection reduces the detection rate by ($\cong 1/10$) times compared to the existing system. The second important conclusion reached is the SNR gain of around 20 dB (for a BER 1×10^{-4} in Fig.5.9) obtained by using macroscopic diversity systems. All these conclusions obtained are based on the restrictions described in Chapter 5.

OFDM is likely to find a range of further attractive applications in wireless and wireline communications. Some of the future research topics are summarized in the following.

a) Coding Modes: This thesis is limited to considering the performance and simulation for non-coded systems. Future research including error control coding can be included with the adaptive modulation system.

b) MIMO/OFDM: OFDM with adaptive modulation can also be applied to Multiple-Input Multiple-Output (MIMO) systems. The same procedure of analyzing constant rate and power to adaptive rate and power techniques in terms of the BER performance can be carried out. Further, the performance of the system can be improved by using selection diversity as well as other more advance space diversity combining techniques.

APPENDIX A

Matlab Codes

The programs in this appendix are the matlab codes used to plot the figures from Chapter 2 to Chapter 5. The Matlab version used to simulate the codes in this appendix is Matlab 6.5.

1) Program 1.m

```
//This code leads to the generation of Fig.2.1. Effect of Degradation due to Frequency Offset
//Offset
i = -1*4;j = -1*2; k=1;
for beta = i: 0.2:j
degrad (k) = beta + 21.3863;           //degradation equation
deg = degrad (k);
xlabel ('Normalized Linewidth/Subcarrier Spacing'); //label, title & legends
ylabel ('Degradation (db)');
title ('Effect of Frequency Offset');
semilogy (beta, deg, '*'); hold on;
k = k + 1;
end
```

2) Program 2.m

```
// Fig.2.1. Probability Distribution Function of a SC system.
x = -3:0.1:3;
p = raylpdf (x,1);           //Rayleigh Distribution pdf.
y = normpdf (x,0,1); //Gaussian Distribution pdf
plot (x, p, '-');
hold on;
plot (x, y)
xlabel ('Rayleigh/Gaussian variable r,x'); //label, title & legends
ylabel ('Probability distribution');
title ('Gaussian and Rayleigh probability density functions');
text (-1,0.4,'Rayleigh distribution--Single carrier system');
text (-1.5,0.25,'Gaussian distribution');
```

3) Program 3.m

```
//Fig.3.1. BER for MQAM
for SNR=0:0.5:40
BER=(1-0.5)*erfc (sqrt (1.5*(10^(SNR/10))/3));           //M=4(signal constellations)
BER1=0.5*(1-0.25)*erfc (sqrt (1.5*10^(SNR/10)/15));    //M=16(signal constellations)
BER2=0.25*(1-0.2)*erfc (sqrt (1.5*10^(SNR/10)/63));   //M=64(signal constellations)
BER3=0.2*(1-0.11)*erfc (sqrt (1.5*10^(SNR/10)/255)); //M=256(signal constellations)
BERa=0.2*exp (-1.6*(10^(SNR/10))/3);                  //Adaptive MQAM..., k=2
BER1a=0.2*exp(-1.6*(10^(SNR/10))/15);                  //Adaptive MQAM..., k=4
BER2a=0.2*exp(-1.6*(10^(SNR/10))/63);                 //Adaptive MQAM..., k=8
BER3a=0.2*exp(-1.6*(10^(SNR/10))/255);                //Adaptive MQAM..., k=16
hold on;
plot (SNR, BER, '*'); plot(SNR,BER1, '*');plot(SNR,BER2, '*');plot(SNR,BER3, '*');
plot (SNR,BERa, 'o');plot(SNR,BER1a, 'o');plot(SNR,BER2a, 'o');plot(SNR,BER3a, 'o');
xlabel('SNR(db)');ylabel('BER');
text(2,0.75, '*- \rightarrow Standard Formula', 'FontSize', 10);
text(2,0.5, 'o- \rightarrow Approximation', 'FontSize', 10);
end
```

4) Program 4.m

```
// The following codes are for the  $k(\gamma)$  for MQAM: Fig.3.3.Continuous rate Average
//BER, Fig.3.4.Continuous rate Instantaneous BER, Fig.3.5.Discrete rate Average BER,
//Fig.3.6.Discrete rate Instantaneous BER
for SNR = 0:0.1:30
n = log2 (1+((10^(SNR/10))));           //Capacity equation .
m = log2 (1+((10^(SNR/10))/(10^(5.8/10))));
plot (SNR,m, '--');
plot (SNR,n, '--');
hold on;
end
```

5) Program 5.m

```
for SNR=0:1:30
n1=log2(1+((10^(SNR/10)))-0.5;
m1=log2(1+((10^(SNR/10))/(10^(5.8/10)))-0.5;
plot(SNR,m1, '--');
plot(SNR,n1, '--');
hold on
end
```

6) Program 6.m

```
for SNR=0:0.2:40
if(SNR<5)
k=0;
k1=0;
```



```

else
k=(1/1)*((log2(10^((SNR-5)/10)))/(10^0.005)) //Continuous case with threshold
//value of 5dB.
k1=(1/1)*((log2(10^((SNR-5)/10)))/(10^0.0005));
end
plot(SNR,k,'-');
plot(SNR,k1,'-');
hold on;
end
xlabel('SNR(db)');
ylabel('Number of bits for modulation-MQAM');

```

7) Program 7.m

```

for SNR=0:0.1:14 k=0;plot(SNR,k,'-') hold on; end
for SNR=14:0.1:18 k=2;plot(SNR,k,'-') hold on; end
for SNR=18:0.1:22 k=4;plot(SNR,k,'-'); hold on; end
for SNR=22:0.1:27 k=6;plot(SNR,k,'-'); hold on; end
for SNR=27:0.1:32 k=8;plot(SNR,k,'-'); hold on; end
for SNR=32:0.1:37 k=10;plot(SNR,k,'-'); hold on; end
for SNR=37:0.1:40 k=12;plot(SNR,k,'-'); hold on; end
for k=0:0.1:2 SNR=14;plot(SNR,k,'-'); hold on; end
for k=2:0.1:4 SNR=18;plot(SNR,k,'-'); hold on; end
for k=4:0.1:6 SNR=22;plot(SNR,k,'-'); hold on; end
for k=6:0.1:8 SNR=27;plot(SNR,k,'-'); hold on; end
for k=8:0.1:10 SNR=32;plot(SNR,k,'-'); hold on; end
for k=10:0.1:12 SNR=37;plot(SNR,k,'-'); hold on; end
xlabel('SNR(db)'); ylabel('Number of bits for modulation-MQAM');

```

8) Program 8.m

```

for SNR=0:0.1:8 k=0; plot(SNR,k,'-'); hold on; end
for SNR=8:0.1:14 k=2; plot(SNR,k,'-'); hold on; end
for SNR=14:0.1:21 k=4; plot(SNR,k,'-'); hold on; end
for SNR=21:0.1:27 k=6; plot(SNR,k,'-'); hold on; end
for SNR=27:0.1:32 k=8; plot(SNR,k,'-'); hold on; end
for SNR=32:0.1:38 k=10; plot(SNR,k,'-'); hold on; end
for SNR=38:0.1:40 k=12; plot(SNR,k,'-'); hold on; end
for k=0:0.1:2 SNR=8; plot(SNR,k,'-'); hold on; end
for k=2:0.1:4 SNR=14; plot(SNR,k,'-'); hold on; end
for k=4:0.1:6 SNR=21; plot(SNR,k,'-'); hold on; end
for k=6:0.1:8 SNR=27; plot(SNR,k,'-'); hold on; end
for k=8:0.1:10 SNR=32; plot(SNR,k,'-'); hold on; end
for k=10:0.1:12 SNR=38; plot(SNR,k,'-'); hold on; end
xlabel('SNR(db)'); ylabel('Number of bits for modulation-MQAM');
forSNR=0:0.1:14 k=0; BER=(0.02*((2^k)-1))/((10^(SNR/10))*k); plot(SNR,BER,'-');
hold on; end

```

```

forSNR=14:0.1:18 k=2;BER=(0.02*((2^k)-1))/((10^(SNR/10))^k);plot(SNR,BER,'-');
hold on; end
forSNR=18:0.1:22 k=4;BER=(0.02*((2^k)-1))/((10^(SNR/10))^k);plot(SNR,BER,'-');
hold on; end
forSNR=22:0.1:27k=6;BER=(0.02*((2^k)-1))/((10^(SNR/10))^k);plot(SNR,BER,'-');
hold on; end
for SNR=27:0.1:32 k=8; BER=(0.02*((2^k)-1))/((10^(SNR/10))^k);plot(SNR,BER,'-');
hold on; end
for SNR=32:0.1:37k=10;BER=(0.02*((2^k)-1))/((10^(SNR/10))^k);plot(SNR,BER,'-');
hold on; end
for SNR=37:0.1:40k=12;BER=(0.02*((2^k)-1))/((10^(SNR/10))^k);plot(SNR,BER,'-');
hold on; end
for BER=0.0005:0.0001:0.001 SNR=14;plot(SNR,BER,'-');hold on; end
for BER=0.0005:0.0001:0.001 SNR=18;plot(SNR,BER,'-');hold on; end
for BER=0.0005:0.0001:0.001 SNR=22;plot(SNR,BER,'-');hold on; end
for BER=0.0005:0.0001:0.001 SNR=27;plot(SNR,BER,'-');hold on; end

```

9) Program 9.m

```

for BER=0.0005:0.0001:0.001 SNR=32;plot(SNR,BER,'-');hold on; end
for BER=0.0005:0.0001:0.001 SNR=37;plot(SNR,BER,'-');hold on; end
xlabel('SNR(db)'); ylabel('BER');

```

10) Program 10.m

```

for SNR=14:0.1:18 k=2; x=10^(SNR/10); y=(2^k)-1;
C=-log((0.01*y)/(0.2*x))*(y/(1.6*x));plot(SNR,C,'-') hold on end
for C=0:0.05:0.38 SNR=14; plot(SNR,C,'-'); hold on end
for SNR=18:0.1:22 k=4; x=10^(SNR/10); y=(2^k)-1;
C=-log((0.01*y)/(0.2*x))*(y/(1.6*x));plot(SNR,C,'-') hold on end
for C=0.2:0.05:0.7 SNR=18; plot(SNR,C,'-'); hold on end
for SNR=22:0.1:27 k=6; x=10^(SNR/10); y=(2^k)-1;
C=-log((0.01*y)/(0.2*x))*(y/(1.6*x));plot(SNR,C,'-') hold on end
for C=0.4:0.05:0.9 SNR=22; plot(SNR,C,'-'); hold on end
for SNR=27:0.1:32 k=8; x=10^(SNR/10); y=(2^k)-1;
C=-log((0.01*y)/(0.2*x))*(y/(1.6*x)); plot(SNR,C,'-') hold on end
for C=0.5:0.05:1.1 SNR=27; plot(SNR,C,'-'); hold on end
for SNR=32:0.1:37 k=10; x=10^(SNR/10); y=(2^k)-1;
C=-log((0.01*y)/(0.2*x))*(y/(1.6*x)); plot(SNR,C,'-') hold on end
for C=0.6:0.05:1.3 SNR=32; plot(SNR,C,'-'); hold on end
for SNR=37:0.1:40 k=12; x=10^(SNR/10); y=(2^k)-1;
C=-log((0.01*y)/(0.2*x))*(y/(1.6*x)); plot(SNR,C,'-') hold on end
for C=0.6:0.05:1.6 SNR=37; plot(SNR,C,'-'); hold on end
xlabel('Average SNR(dB)');
ylabel('Power ratio');

```

REFERENCE

- [2.1] J. M. Chung, Dongfang Liu, K. Ramasamy, and S. Varadarajan, "OFDM frame synchronization in slotted ALOHA mobile communication systems," *Proc. IEEE VTC'2001*, vol. 3, pp. 1373-1377, Fall 2001.
- [3.1] J. G. Proakis, *Digital Communications*, 3rd ed. NY: McGraw-Hill, 1995.
- [3.2] T. Pollet, M. Van Bladel, M. Moeneclaey, "BER Sensitivity of OFDM Systems to Carrier Frequency Offset and Weiner Phase Noise," *IEEE Transactions on Communications*, vol. 43, pp. 2/3/4, Feb/Mar/Apr 1995.
- [3.3] V. K. Dubley and L. Wan, "Bit error probability of OFDM system over frequency nonselective fast Rayleigh fading channels," *IEEE Electronics Letters*, vol. 36, pp. 1306-1307, 2000.
- [3.4] A. Papoulis, *Probability, random variables, and stochastic processes*, 3rd ed. New York, NY: McGraw-Hill, 1991.
- [4.1] S.T. Chung and A. J. Goldsmith, "Degrees of Freedom in Adaptive Modulation: A Unified View," *IEEE Trans. Commun*, vol. 49, no.9, pp.1561-1571, Sept. 2001.
- [5.1] T. Keller and L. Hanzo, "A Convenient Framework For Time-Frequency Processing in Wireless Communications," *Proc. IEEE*, vol. 88, no.5, pp. 611-640, May 2000.

- [5.2] T. Keller, T. H. Lewis, and L. Hanzo, "Adaptive Redundant Residue Number System Coded Multicarrier Modulation," *IEEE Journal On Selected Areas in Communications*, vol.18, pp. 2292-2301, Nov. 2000.
- [5.3] T. Keller, and L. Hanzo,"Adaptive Modulation Techniques for Duplex OFDM Transmission," *IEEE Transactions On Vehicular Technology*, vol.49, no.5, pp.1893-1906, Sept. 2000.
- [5.4] R. Hermann and G. Rainer, "Performance Comparison of Different Multiple Access Schemes for the Downlink of an OFDM Communication System," *Proc. IEEE ICC'97*, 1997.
- [5.5] T. Pollet, M. Van Bladel, and M. Moeneclaey, "BER Sensitivity of OFDM Systems to Carrier Frequency Offset and Weiner Phase Noise," *IEEE Transactions on Communications*, vol. 43, pp. 2-4, Feb. 1995.
- [5.6] M. Speth, D. Daecke, and H. Meyr, "Minimum Overhead Burst Synchronization for OFDM Based Broadband Transmission," *Proc. IEEE*, pp. 2777- 2782, 1998.
- [5.7] W. T. Webb and R. Steele, "Variable rate QAM for mobile radio," *IEEE Trans. Commun.*, vol. 43, pp. 2223-2230, July 1995.
- [5.8] A. M. D. Turkmani, "Probability of error for M -branch macroscopic selection diversity," *IEE Proceedings-I*, vol. 139, pp. 71-78, Feb. 1992.

∞

VITA

Krishnaveni Ramasamy

Candidate for the Degree of

Master of Science

Thesis: AN INVESTIGATION OF ADAPTIVE CONTROL TECHNIQUE IN
OFDM WIRELESS MODULATION

Major Field: Electrical Engineering

Biographical:

Personal Data: Born in Coimbatore, India on May 27th 1978.

Education: Received a Bachelor of Science in Electrical Engineering from Coimbatore Institute Of Technology, Coimbatore in August 1999. Completed the requirements for the Master of Science degree with a major in Electrical Engineering at Oklahoma State University in December, 2002.

Experience:

- 1) Employed by Oklahoma State University, School of Electrical and Computer Engineering as a research assistant, August 2000 to May 2002.
- 2) Employed by Oklahoma State University, School of Electrical and Computer Engineering as a teaching assistant, January 2000 to May 2002.
- 3) Worked as an Intern in Techrol Inc., Pawnee, OK, May 2002 to July 2002.

THE MOST IMPORTANT CO-LEADER SKILLS
AND TRAITS ON EXTENDED OUTDOOR
EXPEDITIONS AS PERCEIVED
BY LEADERS

By

CHRISTEL RILLING

Bachelor of Science (Agriculture)

University of Guelph

Guelph, Ontario

1990

Submitted to the Faculty of the
Graduate College of the
Oklahoma State University
in partial fulfillment for
the Degree of
MASTER OF SCIENCE
December, 2002